

# MP2 Is Not Good Enough: Transfer Learning ML Models for Accurate VPT2 Frequencies

Silvan Käser, Eric Boittier, Meenu Upadhyay, and Markus Meuwly\*

*Department of Chemistry, University of Basel, Klingelbergstrasse 80 , CH-4056 Basel,  
Switzerland.*

E-mail: [m.meuwly@unibas.ch](mailto:m.meuwly@unibas.ch)

March 15, 2021

## Abstract

The calculation of the anharmonic modes of small to medium sized molecules for assigning experimentally measured frequencies to the corresponding type of molecular motions is computationally challenging at sufficiently high levels of quantum chemical theory. Here, a practical and affordable way to calculate coupled-cluster quality anharmonic frequencies using second order vibrational perturbation theory (VPT2) from machine-learned models is presented. The approach, referred to as “NN + VPT2”, uses a high-dimensional neural network (PhysNet) to learn potential energy surfaces (PESs) at different levels of theory from which harmonic and VPT2 frequencies can be efficiently determined. The NN + VPT2 approach is applied to eight small to medium sized molecules ( $\text{H}_2\text{CO}$ , trans-HONO, HCOOH,  $\text{CH}_3\text{OH}$ ,  $\text{CH}_3\text{CHO}$ ,  $\text{CH}_3\text{NO}_2$ ,  $\text{CH}_3\text{COOH}$  and  $\text{CH}_3\text{CONH}_2$ ) and frequencies are reported from NN-learned models at the MP2/aug-cc-pVTZ, CCSD(T)/aug-cc-pVTZ and CCSD(T)-F12/aug-cc-pVTZ-F12 levels of theory. For the largest molecules and at the highest levels of theory, transfer learning (TL) is used to determine the necessary full-dimensional, near-equilibrium PESs. Overall, NN+VPT2 yields anharmonic frequencies to within  $20\text{ cm}^{-1}$  of experimentally determined frequencies for close to 90 % of the modes for the highest quality PES available and to within  $10\text{ cm}^{-1}$  for more than 60 % of the modes. For the MP2 PESs only  $\sim 60\%$  of the NN+VPT2 frequencies were within  $20\text{ cm}^{-1}$  of the experiment, with outliers up to  $\sim 150\text{ cm}^{-1}$  compared with experiment. It is also demonstrated that the approach allows to provide correct assignments for strongly interacting modes such as the OH bending and the OH torsional modes in formic acid monomer and the CO-stretch and OH-bend mode in acetic acid.

# 1 Introduction

Vibrational spectroscopy is a sensitive probe for identifying molecules or to follow conformational and structural changes in the gas phase and in solution. One essential task in the practical use of vibrational spectroscopy is the assignment of a measured frequency to its corresponding type of molecular motion. Based on this information it is also possible to predict changes both in the characterization of these motions and their influence on the frequencies themselves. In spectrally congested regions, as in the frequency range between  $1200\text{ cm}^{-1}$  and  $1700\text{ cm}^{-1}$ , these assignments are particularly challenging due to couplings between the different degrees of freedom. Similarly, force field parametrization relies on fitting computed normal mode frequencies to the correctly assigned band positions from experiment. In practice it would, however, be preferable to use anharmonic computed frequencies in force field development because normal modes are already based on the harmonic oscillator assumption. It is for such tasks that computational approaches are particularly valuable.

An accurate description of the vibrational dynamics and IR spectroscopy remains a challenging problem in molecular spectroscopy.<sup>1</sup> Often, these calculations require accurate, full-dimensional potential energy surfaces (PESs) for which machine learning (ML) methods have gained a lot of attention.<sup>2</sup> ML potentials are used to generate statistical models for energies and forces based on molecular structures from extensive *ab initio* data. The resulting potentials can reproduce the reference data with unprecedented accuracies<sup>3,4</sup> (energies and forces with errors in the range of  $10^{-2} - 10^{-5}$  kcal/mol and  $10^{-1} - 10^{-3}$  kcal/mol/Å, harmonic frequencies are obtained within  $\sim 0.5\text{ cm}^{-1}$ ) and thus are superior to *ab initio* potentials due to their efficiency.

Predictions of accurate anharmonic frequencies which compare sufficiently well with experiment remain a challenge to overcome and allow assignments of the vibrations and interpretation of spectroscopic features.<sup>5-7</sup> Recent studies<sup>8,9</sup> illustrate that IR spectra determined

from molecular dynamics (MD) simulations are unable to capture the full anharmonic behaviour of the molecule, especially for high-frequency modes. This motivates the search for alternative approaches, given that a sufficient number of reference calculations, at high levels of theory, have become possible.<sup>3,10,11</sup>

This work presents a practical approach to calculate anharmonic frequencies from accurate, machine-learned potentials for small (4 atoms) to medium-sized (9 atoms) molecules. The ML-PESs are used as an external energy function to quantum chemistry software (here the Gaussian package<sup>12</sup>), to determine energies, forces, force constants, dipole moments and dipole moment derivatives for a vibrational perturbation theory (VPT2) analysis.<sup>13</sup> This has the advantage that a direct comparison of results from explicit normal mode and VPT2 calculations, at a given level of theory from the electronic structure code, and the results from using the ML-PES is possible. Moreover, ML models can be systematically improved by including additional data and/or by using data from higher levels of quantum chemical theory. For this, transfer learning (TL) schemes, which have been shown to be data-efficient alternatives,<sup>3,14,15</sup> can be used to achieve higher quality PESs and will be explored here, too.

The present work reports on a systematic study of anharmonic frequencies for H<sub>2</sub>CO, trans-HONO, HCOOH, CH<sub>3</sub>OH, CH<sub>3</sub>CHO, CH<sub>3</sub>NO<sub>2</sub>, CH<sub>3</sub>COOH and CH<sub>3</sub>CONH<sub>2</sub> based on machine-learned models employing reference data from electronic structure calculations at different levels of theory. The machine-learned models will then be used for harmonic and VPT2 calculations which can also be compared with results from experiments. Furthermore, TL to higher levels of theory is explored. As an example, for the largest molecules a sufficient number of energies and forces (estimated to be around 10<sup>4</sup> or larger) at the highest levels of theory, such as CCSD(T), is usually not feasible. Hence, a relevant question is whether by starting from a robust MP2-learned PES one can ‘transfer learn’ to a CCSD(T)-quality PES from a considerably smaller set of reference energies and gradients at this higher level

of theory which also yields improved anharmonic frequencies compared with the MP2 level. Earlier work suggests that TL can result in substantial improvements in accuracy and data-efficiency.<sup>3</sup> Finally, the study will also discuss how the cost for generating an accurate ML model (i.e. the cost of structure sampling, training and evaluating the ML model) compares with a single, 'straight' *ab initio* VPT2 calculation.

First, the methods and data generation strategies are presented. This is followed by an assessment of the harmonic and anharmonic modes from the ML-PESs compared with reference electronic structure calculations at different levels of theory. Also, where available, comparison with experimental results is made. Then, the computational efficiency of the approach chosen is considered. Finally, the results are discussed in a broader context and conclusions are drawn.

## 2 Computational Methods

### 2.1 Data sets: sampling and quantum chemical methods

Data sets at three levels of theory, including MP2/aug-cc-pVTZ,<sup>16,17</sup> CCSD(T)/aug-cc-pVTZ,<sup>17-19</sup> and CCSD(T)-F12/aug-cc-pVTZ-F12<sup>20,21</sup> (referred to as "MP2", "CCSD(T)", and "CCSD(T)-F12" for convenience in the following), were generated. All single point electronic structure calculations, including energies, forces and dipole moments required for ML, as well as harmonic frequency calculations, were carried out using MOLPRO.<sup>22</sup> Data sets at the MP2 level of theory were generated for all molecules, for CCSD(T) they were generated for molecules with  $N_{\text{atom}} \leq 6$ , and data sets at the CCSD(T)-F12 level of theory were generated for molecules with  $N_{\text{atom}} \leq 5$ .

As molecules of different sizes are considered, the number of *ab initio* calculations for the data base was scaled accordingly. Here,  $(3N - 6) \cdot 600$  geometries were sampled for each

molecule and the optimized geometry was added. Generation of the reference geometries was based on normal mode sampling:<sup>23</sup> First, the molecules were optimized at the MP2 level of theory, and the normal mode vectors were determined alongside with the corresponding harmonic force constants. Then, distorted (non-equilibrium) conformations were obtained by randomly displacing the atoms along linear combinations of normal mode vectors. This sampling was carried out at different temperatures (here  $T = 10, 50, 100, 300, 500, 1000, 1500$  and  $2000$  K). The total number of geometries was evenly divided between the temperatures, i.e.  $((3N - 6) \cdot 600)/8$  geometries were generated for each  $T$ .

For three molecules, HONO, CH<sub>3</sub>CHO and CH<sub>3</sub>COOH, the initial data set was enlarged by including additional geometries as the PhysNet models predicted normal mode frequencies with larger errors than for the other molecules. For HONO, an additional 2805 structures were added. The geometries were sampled from *NVT* simulations run at 1000 K using the semiempirical GFN2-xTB method<sup>24</sup> and extended with structures along particular normal modes. Moreover, because the structures evaluated in the VPT2 calculations (i.e. the atoms are slightly displaced from the equilibrium geometry for the calculation of numerical derivatives) can be extracted, these were added as well (henceforth, "VPT2 geometries"). For CH<sub>3</sub>CHO, a total of 1072 additional structures were added. These correspond to VPT2 geometries and geometries along particular normal modes. For CH<sub>3</sub>COOH, 109 additional, VPT2 geometries are added.

## 2.2 Machine learning: PhysNet

The representation of the PESs is based on a neural network (NN) using the PhysNet architecture.<sup>25</sup> A detailed description of the NN architecture is given in Reference 25 and only the salient features and those used in the present work are given below. PhysNet is a high-dimensional NN of the "message passing" type<sup>26</sup> and was applied recently to different

molecular systems.<sup>3,27-31</sup> The NN learns a feature vector that encodes the local chemical environment of each atom  $i$  for the prediction of total molecular energies, atomic forces and molecular dipole moments. The feature vector initially contains information about the nuclear charges  $Z_i$  and Cartesian coordinates  $\mathbf{r}_i$  and is iteratively refined (“learned”) during training. The total energy of a molecule with arbitrary geometry includes long-range electrostatics and dispersion interactions and is given by

$$E = \sum_{i=1}^N E_i + k_e \sum_{i=1}^N \sum_{j>i}^N \frac{q_i q_j}{r_{ij}} + E_{D3}. \quad (1)$$

where  $E_i$  are the atomic energy contributions,  $E_{D3}$  is Grimme’s D3 dispersion correction,<sup>32</sup>  $q_i$  are partial charges,  $r_{ij}$  are interatomic distances,  $k_e$  is Coulomb’s constant and  $N$  is the total number of atoms. Note that the partial charges are adjusted to assure charge conservation and the Coulomb term is damped for short distances to avoid numerical instabilities, see Ref. 25 for details. Besides the energy, PhysNet also predicts molecular dipole moments from partial charges according to  $\boldsymbol{\mu} = \sum_{i=1}^N q_i \mathbf{r}_i$  and analytical derivatives of  $E$  with respect to the Cartesian coordinates of the atoms are obtained by reverse mode automatic differentiation.<sup>33</sup>

For the present work, PhysNet was adapted to additionally predict analytical derivatives of the dipole moment  $\boldsymbol{\mu}$  and second order derivatives of  $E$  with respect to Cartesian coordinates (i.e. Hessians). This was easily achieved using Tensorflow<sup>34</sup> utilities.

The data sets containing  $(3N - 6) \cdot 600 + 1$  data points were split according to 85/10/5 % into training/validation/test sets for the fitting of the ML model. The training set always contained the optimized geometry. PES representations are obtained by adapting the PhysNet parameters to best describe reference energies, forces, and dipole moments from explicit quantum chemical calculations. The optimization is carried out using AMSGrad.<sup>35</sup> The relative contribution of the different error terms is controlled by weighting hyperparameters

giving the force error a higher weight/importance compared to the energy error. All hyperparameters of the NN architecture and its optimization approach were set to the values presented in Reference 25, except for the cutoff radius  $r_{\text{cut}}$  for interactions in the NN which was set to 6 Å. Such a cutoff was sufficient to include all interactions in all molecules.

### 2.3 Vibrational second-order perturbation theory

Second-order vibrational perturbation theory (VPT2) is used to include anharmonic and mode coupling effects into spectroscopic properties.<sup>36</sup> Many of the common quantum chemistry packages, such Gaussian<sup>12,13</sup> or CFOUR,<sup>37</sup> include implementations for the calculation of infrared frequencies and intensities including anharmonic effects directly from *ab initio* data. VPT2 assumes that the potential energy of a system can be expressed as a quartic force field given by

$$V = \frac{1}{2} \sum \omega_i \hat{q}_i^2 + \frac{1}{3!} \sum \phi_{ijk} \hat{q}_i \hat{q}_j \hat{q}_k + \frac{1}{4!} \sum \phi_{ijkl} \hat{q}_i \hat{q}_j \hat{q}_k \hat{q}_l. \quad (2)$$

Here,  $\omega_i$  is a harmonic frequency,  $\hat{q}_i$  are (reduced dimensionless) normal mode coordinates, not to be confused with the partial charges  $q_i$ , and  $\phi_{ijk}$  and  $\phi_{ijkl}$  are third- and fourth-order derivatives of the potential  $V$  with respect to normal mode coordinates.<sup>13,38</sup> The first term in Equation 2 corresponds to the harmonic part of the potential while the remaining terms describe anharmonic effects. Using expressions from earlier work<sup>13,38-40</sup> and omitting kinetic/rotational terms, the cubic and quartic force constants can be used to obtain



anharmonic constants:

$$16\chi_{ii} = \phi_{iiii} - \sum_j \frac{(8\omega_i^2 - 3\omega_j^2) \phi_{iij}^2}{\omega_j (4\omega_i^2 - \omega_j^2)} \quad (3)$$

$$4\chi_{ij} = \phi_{iijj} - \sum_k \frac{\phi_{iik} \phi_{jjk}}{\omega_k^2} + \sum_k \frac{2\omega_k (\omega_i^2 + \omega_j^2 - \omega_k^2) \phi_{ijk}^2}{\Delta_{ijk}} \quad (4)$$

$$\Delta_{ijk} = (\omega_i + \omega_j - \omega_k) (\omega_i + \omega_j + \omega_k) (\omega_i - \omega_j + \omega_k) (\omega_i - \omega_j - \omega_k) \quad (5)$$

From the resulting anharmonic constants  $\chi$  the anharmonic fundamental frequencies  $\nu_i$  are obtained according to

$$\nu_i = \omega_i + 2\chi_{ii} + \frac{1}{2} \sum_{i \neq j} \chi_{ij}. \quad (6)$$

In addition, overtones, combination bands and zero-point energies can be determined, see e.g. Ref. 38.

In this work, the generalized VPT2<sup>13</sup> implementation (GVPT2) in the Gaussian<sup>12</sup> suite is used to determine anharmonic frequencies. Specific settings including which VPT2 model to use, step-size for numerical differentiation and resonance thresholds are retained at their default values. Gaussian’s standardized interface initialized by the “External” keyword is used to call an external script (i.e. the PhysNet potential), which produces an energy, gradients and Hessians for a given molecule/geometry. The output from the external potential is recovered from a standard text file by Gaussian where the the cubic and quartic terms are determined by numerical derivatives and used for a VPT2 calculation.

### 3 Results

The performance of the ML models is assessed by three points: i) Out-of-sample errors for energies ( $\Delta E$ ) and forces ( $\Delta F$ ) for which geometries of a separate test set are used. These errors quantify to what extent the ML models are capable of interpolating between training points. ii) Comparing harmonic frequencies determined from the trained PhysNet model and conventional *ab initio* harmonic frequencies calculations at the same level of theory. These harmonic frequencies also affect the anharmonic (VPT2) frequencies, see Eq. 6), and iii) Comparing VPT2 frequencies from the PhysNet model with those from Gaussian at the MP2 level of theory and with those from experiment, respectively. The comparison with *ab initio* MP2 VPT2 frequencies quantifies how closely the PhysNet PES reproduces the *ab initio* potential around the minimum.

#### 3.1 Out-of-sample errors

All the PhysNet models were evaluated on separate test sets by means of MAEs and root mean squared errors (RMSEs) for energies and forces between reference calculations and predictions by PhysNet, see Figures 1 and 2. MAEs (squares) and the RMSEs (triangles) at different levels of theory are color coded. For each of the molecules and levels of theory two independent PhysNet models (opaque and transparent symbols) were trained on the same data to assess consistency and reproducibility. The lowest MAE( $E$ ) is  $\approx 0.0005$  kcal/mol (for H<sub>2</sub>CO) whereas the largest is  $\approx 0.0218$  kcal/mol (for CH<sub>3</sub>CONH<sub>2</sub>) indicating that errors scale with system size. These MAEs correspond to about 0.003 and 0.03 % of the energy range spanned by the data sets (16.3 kcal/mol for H<sub>2</sub>CO and 72.6 kcal/mol for CH<sub>3</sub>CONH<sub>2</sub>), respectively, and all  $R^2$  coefficients are above 0.99998 (see Table S2). From Figure 1 it is apparent that two independently trained models (opaque and transparent symbols on the same vertical line) can still differ appreciably (MAEs( $E$ ) of  $\sim 0.0013$  and  $\sim 0.0072$  kcal/mol

for  $\text{H}_2\text{CO}$  trained on MP2 data, see Tab. S2) although both models are still of remarkable quality.

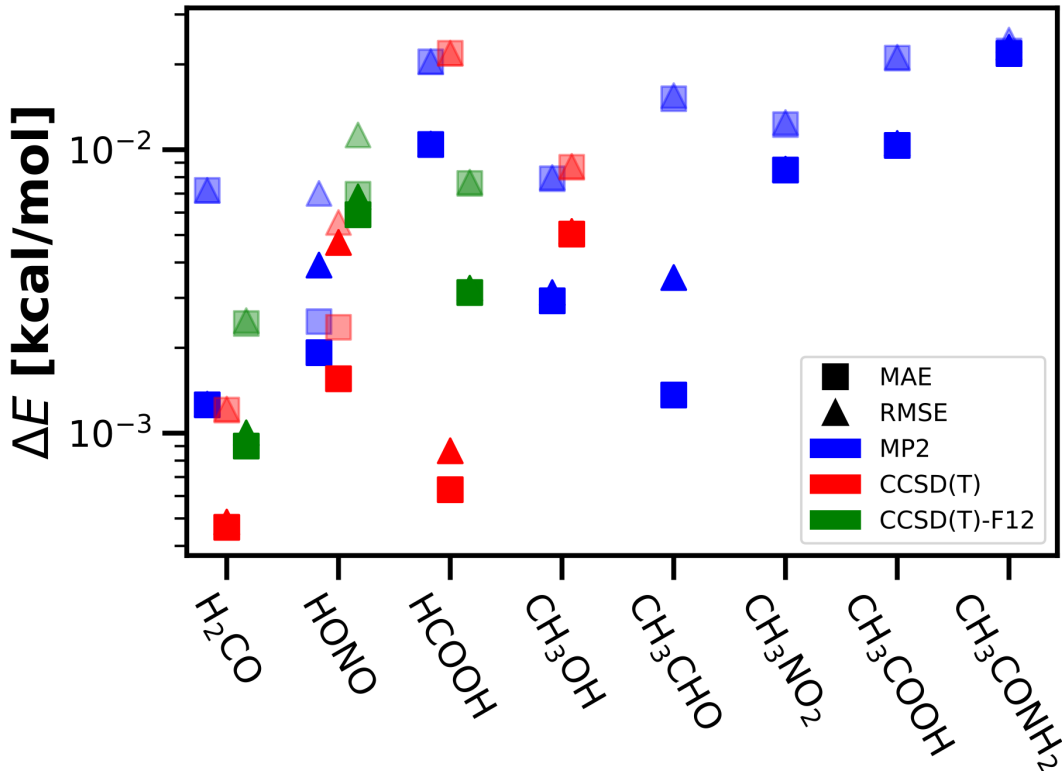


Figure 1: The out-of-sample MAEs (squares) and RMSEs (triangles) of the energy for the different molecules. The levels of theory are color-coded and opaque and transparent symbols represent two PhysNet models trained independently on the same data. A general trend showing an increased error with increasing system size is visible. The lowest MAE is  $\sim 0.0005$  kcal/mol ( $\text{H}_2\text{CO}$ , CCSD(T)) and the highest is  $\sim 0.0218$  kcal/mol ( $\text{CH}_3\text{CONH}_2$ , MP2). All PhysNet models predict the independent test set with chemical accuracy (better than 1 kcal/mol) and all out-of-sample performance measures are summarized in Table S2.

The appreciable variations between the two models trained on the same data (opaque and transparent symbols, respectively) are notably smaller for the force errors (i.e. the opaque and transparent squares are very close to each other),  $\text{MAE}(F)$  and  $\text{RMSE}(F)$ , see Figure 2. Earlier work<sup>3</sup> showed that this is a consequence of the different weights (hyperparameters) in the loss function of PhysNet. During training, the higher weight of the force leads to a

slight deterioration of the energies while the forces are still improving. The higher weight on the forces, however, is motivated by the fact that accurate derivatives are required for the present work. Similar to the errors in the energies  $\Delta E$ , the force errors  $\Delta F$  tend to increase with increasing system size. The force errors for H<sub>2</sub>CO are notably lower compared to the other molecules. Because PhysNet is invariant with respect to permutation of equivalent atoms, the C<sub>2v</sub> symmetry of H<sub>2</sub>CO could be responsible for the lower out-of-sample errors. All test sets are predicted with energy errors considerably better than chemical accuracy and, according to earlier studies using PhysNet, are within the expected range (see e.g. Refs. 3 and 29 for H<sub>2</sub>CO and for larger molecules, respectively).

### 3.2 Harmonic frequencies

Harmonic frequencies computed from the PhysNet representations are useful to test how well the ML model reproduces the region close to the minimum of the PES compared with frequencies determined directly from the *ab initio* calculations. Also, they provide the anharmonic frequencies through Eq. 6 which will be essential for the calculation of VPT2 frequencies. Figure 3 compares the reference *ab initio* harmonic frequencies from MOLPRO<sup>22</sup> with those from PhysNet after optimizing the structure of each molecule with the respective energy function. From the two models trained independently on the same data, only the frequencies from the best PhysNet model are discussed. The complete list of PhysNet and *ab initio* harmonic frequencies for all molecules and at all levels of theory are reported in Tables S3-S5, S7-S9, S11-S13, S15, S16, S18, S20, S22, and S24.

For the smaller molecules (Figure 3A), all harmonic frequencies from the PhysNet models are within 1 cm<sup>-1</sup> (mostly < 0.5 cm<sup>-1</sup>) of the reference *ab initio* calculations and the MAEs( $\omega$ ) range from 0.08 to 0.21 cm<sup>-1</sup>. Similarly, for the larger molecules (Figure 3B) most of the harmonic frequencies are within 1 cm<sup>-1</sup> of the reference values. Single larger differ-

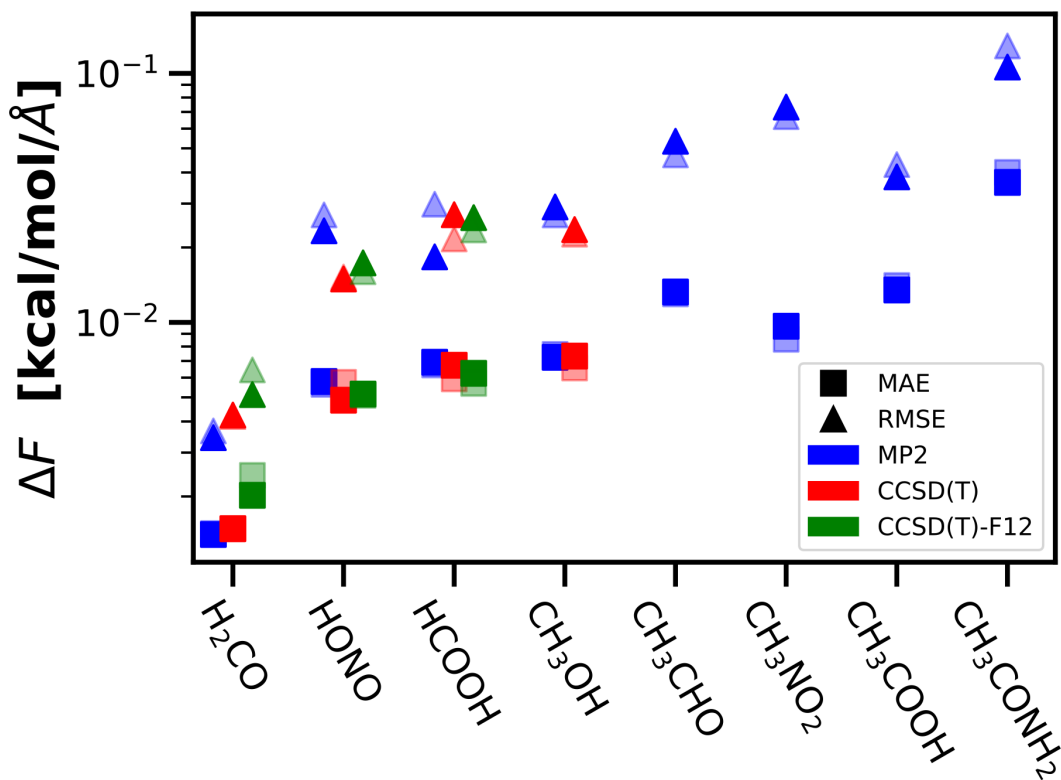


Figure 2: The out-of-sample MAEs (squares) and RMSEs (triangles) of the forces for the different molecules. The levels of theory are color-coded, and the opaque and transparent symbols represent two PhysNet models trained independently on the same data. A general trend showing an increased error with increasing system size is visible. The lowest MAE is  $\sim 0.0013$  kcal/mol/Å (H<sub>2</sub>CO, MP2) and the highest is  $\sim 0.0400$  kcal/mol/Å (CH<sub>3</sub>CONH<sub>2</sub>, MP2). All out-of-sample performance measures can be found in Tab. S2.

ences are found for the low frequency modes with errors of 1.23 and 2.01  $\text{cm}^{-1}$  for CH<sub>3</sub>NO<sub>2</sub> and CH<sub>3</sub>CONH<sub>2</sub>, respectively. The remaining PhysNet frequencies reproduce the *ab initio* harmonic frequencies with errors smaller than 1  $\text{cm}^{-1}$  and MAEs( $\omega$ ) are between 0.09 and 0.28  $\text{cm}^{-1}$ . Note that all the optimized structures are true minima (i.e. no imaginary frequencies were found).

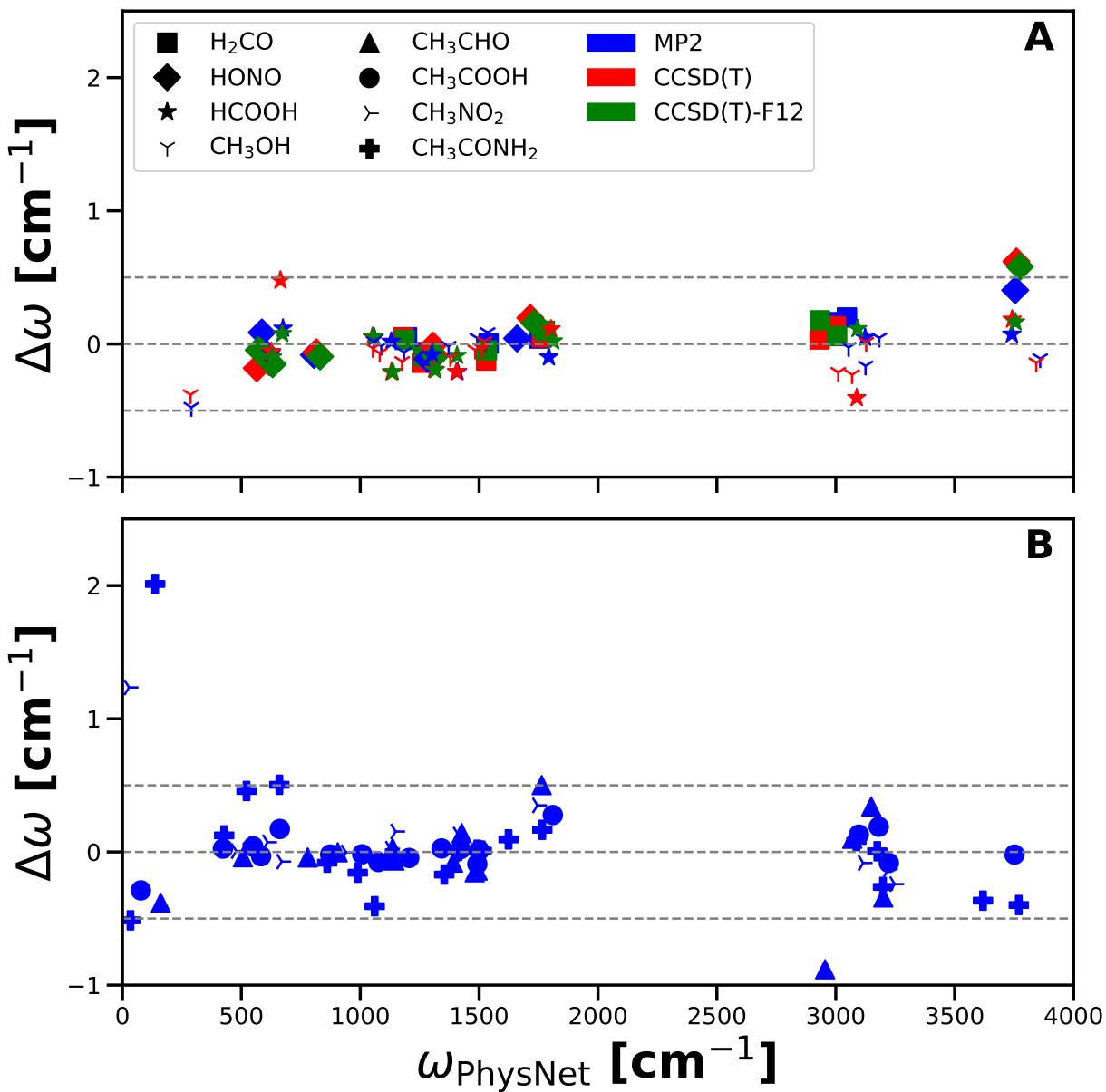


Figure 3: The accuracy of the PhysNet harmonic frequencies is shown with respect to the appropriate reference *ab initio* values. Here,  $\Delta\omega$  corresponds to  $\omega_{\text{ref}} - \omega_{\text{PhysNet}}$  and the figure is divided into two windows for clarity. For the small molecules (A), irrespective of the level of theory, all frequencies are reproduced to within less than 1 cm<sup>-1</sup>. For the larger molecules (B), deviations larger than 1 cm<sup>-1</sup> are found. Largest errors are found for CH<sub>3</sub>NO<sub>2</sub> (1.23 cm<sup>-1</sup>) and for CH<sub>3</sub>CONH<sub>2</sub> (2.01 cm<sup>-1</sup>). Tables containing the PhysNet and *ab initio* harmonic frequencies can be found in Tabs. S3-S5, S7-S9, S11-S13, S15, S16, S18, S20, S22, S24.

### 3.3 VPT2 frequencies

Next the quality of the VPT2 frequencies for the best (based on the  $\text{MAE}(\nu)$ ) PhysNet models is assessed. For this, VPT2 frequencies computed from PhysNet models trained on MP2 data are compared to their *ab initio* counterparts, see Figure 4. This comparison was not done for the higher levels of theory because the VPT2 method in Gaussian is only available for levels with analytical second derivatives<sup>12</sup> and because the calculations get very expensive for the larger molecules. The majority of the MP2 VPT2 frequencies are reproduced to within better than  $5 \text{ cm}^{-1}$  with single larger differences of up to  $\sim 10 \text{ cm}^{-1}$ . It is apparent that the PhysNet VPT2 frequencies for the smaller molecules (Figure 4A) are more accurate - with  $\text{MAEs}(\nu)$  between  $0.95$  and  $1.55 \text{ cm}^{-1}$  - than the frequencies of the larger molecules (Figure 4B). For the larger molecules  $\text{MAEs}(\nu)$  between  $1.14$  and  $2.71 \text{ cm}^{-1}$  are found. The good agreement between *ab initio* and PhysNet VPT2 frequencies further confirms the high quality of the ML potentials as third and fourth order derivatives of the potential are very sensitive to the shape and accuracy of the PES. Note that for two molecules ( $\text{CH}_3\text{NO}_2$  and  $\text{CH}_3\text{CONH}_2$ ) one and two negative VPT2 frequencies are found for the lowest frequency modes from PhysNet as well as from the *ab initio* calculations. This is a deficiency of VPT2 and can be explained by Equation 6. If the perturbation  $2\chi_{ii} + \frac{1}{2} \sum_{i \neq j} \chi_{ij}$  exceeds the harmonic frequency  $\omega_i$  (and is negative), which can occur in particular for small  $\omega_i$ , the VPT2 frequency can become negative. These frequencies are reported in Tables S23 and S25. Even though a direct comparison of the higher level PhysNet VPT2 to the *ab initio* reference is intractable, it seems reasonable to assume that the coupled cluster quality PhysNet models reach similar accuracies. This is further supported by the findings for the harmonic frequencies at the CCSD(T) and CCSD(T)-F12 levels.

The (anharmonic) PhysNet VPT2 frequencies can also be compared directly to experimental data, see Figure 5. For the small molecules good agreement is found and the frequencies converge towards the experimental values when going from MP2 to CCSD(T)-F12.

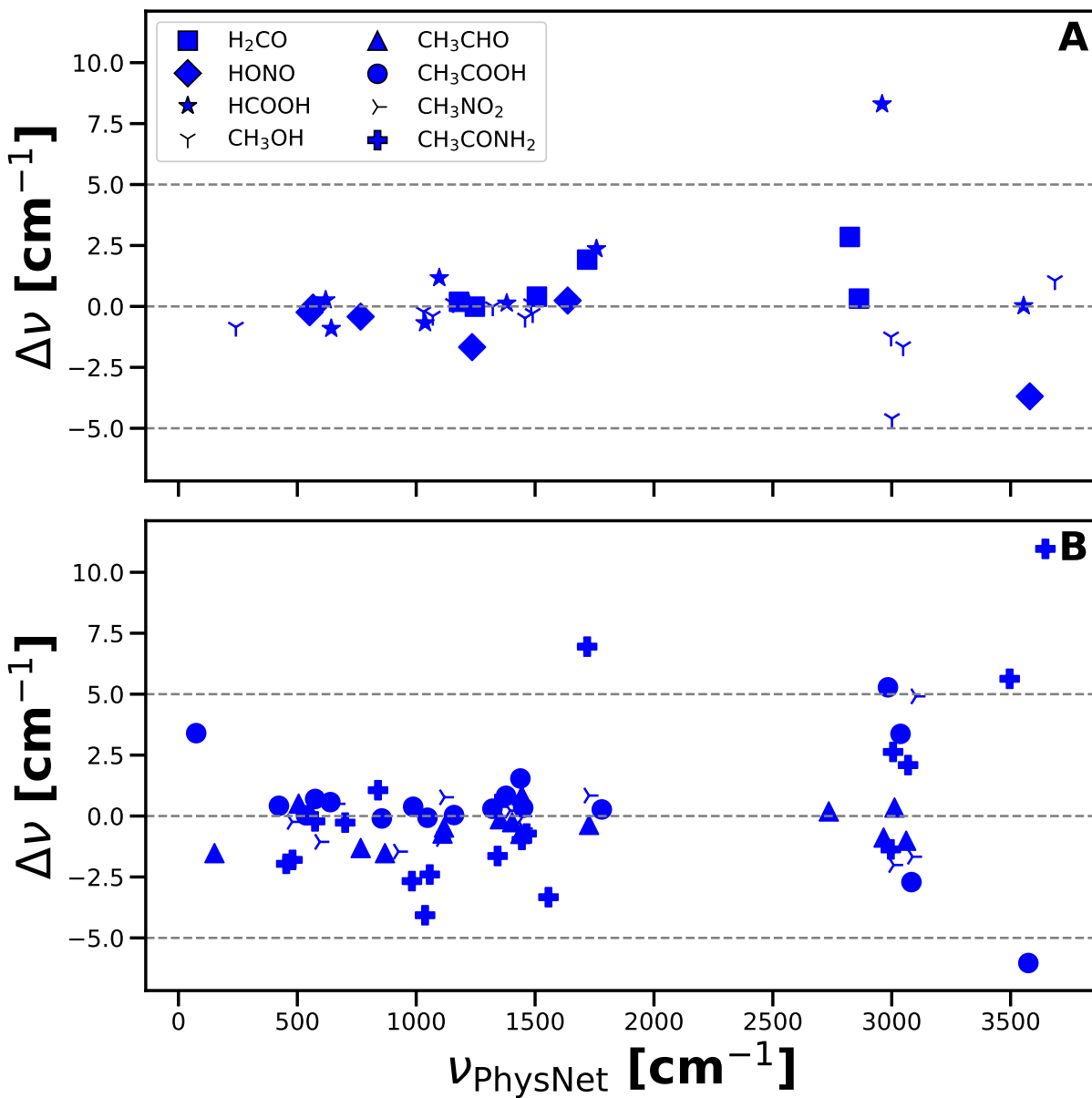


Figure 4: The accuracy of the PhysNet MP2 VPT2 frequencies is shown with respect to their MP2 *ab initio* values. Here,  $\Delta\nu$  corresponds to  $\nu_{\text{MP2}} - \nu_{\text{PhysNet}}$  and the figure is divided into two windows for clarity. For most of the molecules and frequencies, the reference anharmonic frequencies are reproduced with deviations smaller than  $10 \text{ cm}^{-1}$  (or even  $5 \text{ cm}^{-1}$  for the small molecules). The anharmonic frequencies of CH<sub>3</sub>NO<sub>2</sub> and CH<sub>3</sub>CONH<sub>2</sub> having negative frequencies are not shown. Tables containing the PhysNet and *ab initio* VPT2 frequencies can be found in Tabs. S6, S10, S14, S17, S19, S21, S23, S25.

VPT2 frequencies from the PhysNet model for H<sub>2</sub>CO trained on CCSD(T)-F12 data reproduce the experimental data<sup>41</sup> with a maximum deviation of  $\sim 20 \text{ cm}^{-1}$  and a  $\text{MAE}(\nu)$



of  $\sim 4 \text{ cm}^{-1}$ . Similar trends are also visible for the other CCSD(T)-F12 models where a  $\text{MAE}(\nu)$  of  $\sim 7 \text{ cm}^{-1}$  ( $\sim 4 \text{ cm}^{-1}$ ) is found for HONO (HCOOH), see Table 1. In going from MP2 to CCSD(T)-F12 the MAE reduces by a factor of almost five. For CH<sub>3</sub>OH the highest quality PhysNet model is trained on CCSD(T) reference calculations. Here, larger deviations of up to  $\sim 58 \text{ cm}^{-1}$  for single vibrations and a  $\text{MAE}(\nu) = 14.30 \text{ cm}^{-1}$  are found.

For the larger molecules (Figure 5B) the PhysNet models are only trained on MP2 reference data. As judged from the improvements between VPT2 calculations at the MP2, CCSD(T), and CCSD(T)-F12 levels with experiment for H<sub>2</sub>CO, HONO and HCOOH, for PhysNet trained on MP2 data only modest agreement between computed and experimentally observed frequencies is expected for the larger molecules. VPT2 modes from the PhysNet models trained on MP2 data for the larger molecules (Figure 5B) with frequencies below  $\sim 2000 \text{ cm}^{-1}$  are centered around the experimental values with a  $\text{MAE}(\nu)$  between 6 and  $30 \text{ cm}^{-1}$ . The higher frequencies, however, tend to be overestimated by PhysNet trained on data at the MP2 level of theory ( $\text{MAE}(\nu)$  between 31 and  $97 \text{ cm}^{-1}$ ). Because VPT2 frequencies from PhysNet and *ab initio* MP2 calculations agree well (see Figure 4) it is concluded that the (large) errors are not caused by the ML method itself but rather are a deficiency of the MP2 level of theory and/or of the VPT2 approach when compared with experiment. Nevertheless, for completeness, the MAEs with respect to experiment are given in Table 1. As it becomes computationally unfeasible to calculate a comprehensive CCSD(T) data set containing some thousand data points for the larger molecules, an alternative approach to improve the ML models is required. This is explored next.

### 3.4 Transfer learning to coupled cluster quality

As the accuracy of the MP2 based models is limited and as it is computationally too expensive to obtain comprehensive coupled cluster quality training data sets for the larger

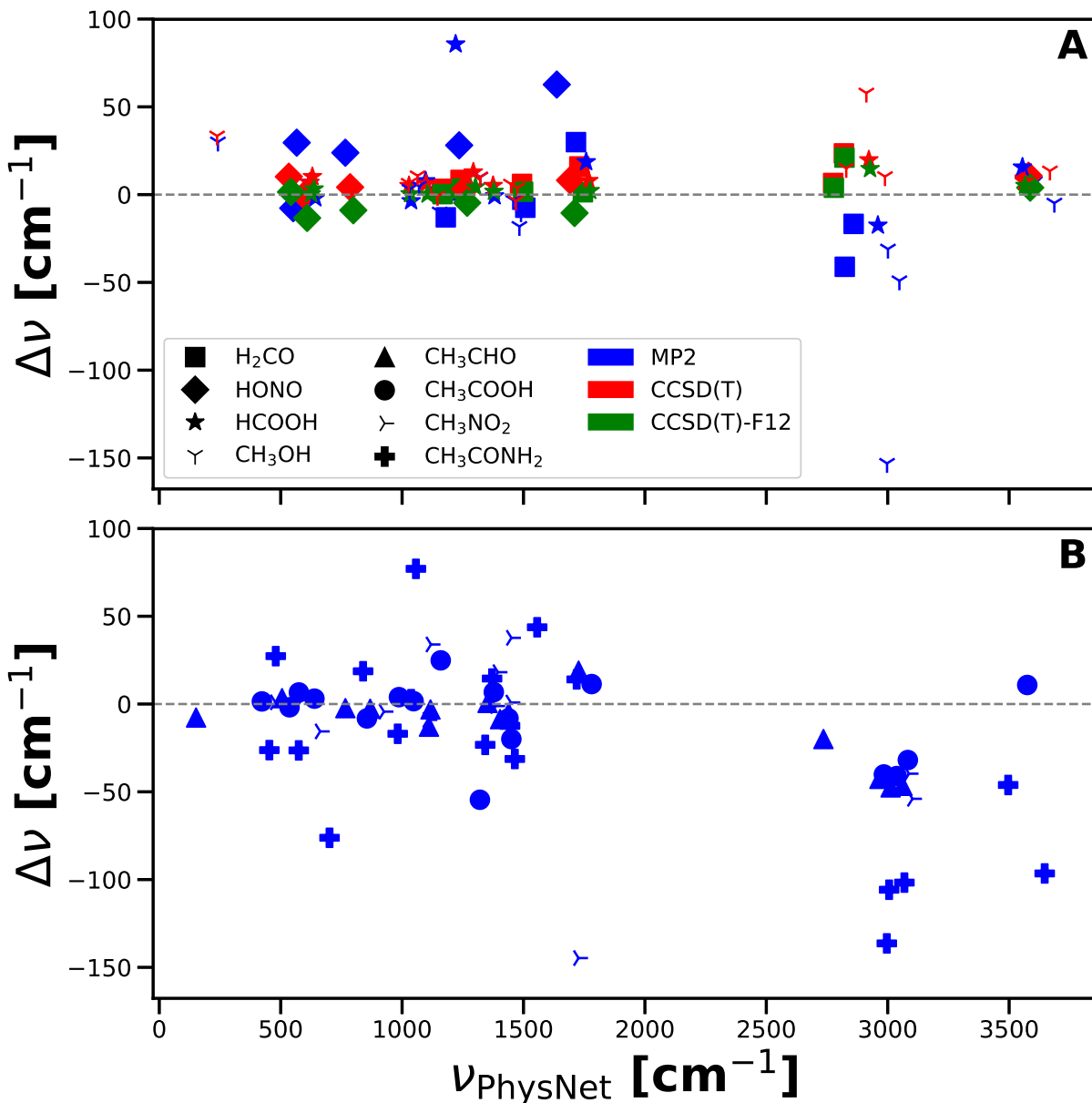


Figure 5: VPT2 frequencies from PhysNet compared with experimental values.<sup>41–48</sup> Here,  $\Delta\nu = \nu_{\text{exp}} - \nu_{\text{PhysNet}}$  and the figure is divided into two panels for smaller (panel A) and larger (panel B) molecules. For H<sub>2</sub>CO good agreement is achieved with experiment, where the frequencies converge towards the experiment going from MP2 to CCSD(T)-F12 with a maximum deviation of  $\sim 20 \text{ cm}^{-1}$ . A similar trend is also visible for HCOOH and CH<sub>3</sub>OH. In panel B, larger deviations are visible especially for high frequencies. Tables S6, S10, S14, S17, S19, S21, S23, S25 report the PhysNet, MP2 *ab initio* VPT2, and experimental frequencies. For HCOOH the literature suggests different frequencies for the OH bending mode, see Refs.<sup>43,49</sup> (1229 and 1302  $\text{cm}^{-1}$ , respectively). Here, a frequency of 1302 is used, following Ref. 43.

molecules, alternative methods have to be considered. Among NN based methods TL can be used to exploit correlations between data at different levels of theory.<sup>50</sup> TL uses the knowledge, acquired when learning how to solve a task A, as a starting point to learn how to solve a related, but different task B.<sup>14,15</sup> Methods related to TL are  $\Delta$ -machine learning<sup>51</sup> or multi-fidelity learning<sup>52</sup> which become increasingly popular in quantum chemical applications.<sup>29,50,53,54</sup> Also, TL bears similarities with potential morphing techniques which exploit the fact that the overall shapes of PESs at sufficiently high levels of theory are related and can be transformed by virtue of suitable coordinate transformations.<sup>55,56</sup>

Here, TL is used to obtain coupled cluster quality PESs for the larger molecules based on models trained at the MP2 level. For this, the MP2 models are used as a good initial guess and only a fraction of the data set, calculated at the CCSD(T) level, needs to be provided for TL. To transfer learn the models, the parameters of a PhysNet model trained on MP2 data is used to initialize the PhysNet training. Then, PhysNet is trained (i.e. the parameters are adjusted) using energies, forces and dipole moments from the higher level of theory. The training is performed following the same approach and using the same hyperparameters as when training a model from scratch, except that the learning rate is decreased to values between  $10^{-5} - 10^{-4}$ .

First, TL is applied to H<sub>2</sub>CO which serves as a “toy model” because PhysNet models at different levels of theory are readily available and allow for direct comparison. In other words, the TL model based on MP2 data and retrained with input from CCSD(T)-F12 can be directly compared with PhysNet trained entirely on CCSD(T)-F12 reference data. For this, the MP2 model is used as initial guess and transfer learned to CCSD(T)-F12 quality using 188 data points (151 of the original data set extended with 37 VPT2 geometries) and tested on the remaining 3450 structures from the original CCSD(T)-F12 data set. The TL model shows slightly lower errors for energies ( $\text{MAE}(E) = 0.0004 \text{ kcal/mol}$ ) compared to the

model trained from scratch ( $\text{MAE}(E) = 0.0009 \text{ kcal/mol}$ ), whereas the forces are slightly less accurate with  $\text{MAE}(F)$  of 0.0066 and 0.0020 kcal/mol/Å for TL and from scratch, respectively. For the harmonic frequencies, all reference CCSD(T)-F12 values are reproduced with deviations smaller than  $0.3 \text{ cm}^{-1}$  and with a  $\text{MAE}(\omega) = 0.1 \text{ cm}^{-1}$ , which is similar for a model trained from scratch, see Tables S5 and S26. The most relevant measure of performance is the direct comparison of VPT2 to experimental frequencies, especially when the high level *ab initio* calculation of harmonic frequencies become too expensive. Figure 6 shows the deviation of a transfer learned PhysNet model, a PhysNet model trained on CCSD(T)-F12 data and a model trained on MP2 data (the “base model” for TL) with respect to the experimental H<sub>2</sub>CO frequencies. VPT2 frequencies from NN<sub>TL</sub> are very close to those from NN<sub>CCSD(T)-F12</sub> except for one high frequency mode and clearly superior to those from NN<sub>MP2</sub> throughout when compared with experiment.

TL is used to obtain high quality PESs for all the models for which only MP2 reference data are available (i.e. CH<sub>3</sub>CHO, CH<sub>3</sub>NO<sub>2</sub>, CH<sub>3</sub>COOH and CH<sub>3</sub>CONH<sub>2</sub>). For each of the molecules around 5 % or less of the original, lower level, data set is recalculated at the CCSD(T) level. The TL data sets contain geometries sampled using the normal mode approach (evenly split among the different temperatures), VPT2 geometries and the MP2 optimized geometry. They contained CCSD(T) information (energies, gradients and dipole moments) on 262, 452, 542 and 632 CCSD(T) geometries for CH<sub>3</sub>CHO, CH<sub>3</sub>NO<sub>2</sub>, CH<sub>3</sub>COOH and CH<sub>3</sub>CONH<sub>2</sub>, respectively. The TL data sets are again split randomly according to 85/10/5 % into training/validation/test sets for TL. As a consequence, the TL models are tested only on a small number of molecular geometries.

For the larger molecules assessing the performance of a TL model is more difficult. On the one hand, the rather small number of geometries in the TL set are mostly used for training and validation. Thus, only a small fraction ( $< 50$  geometries) remains for testing the mod-

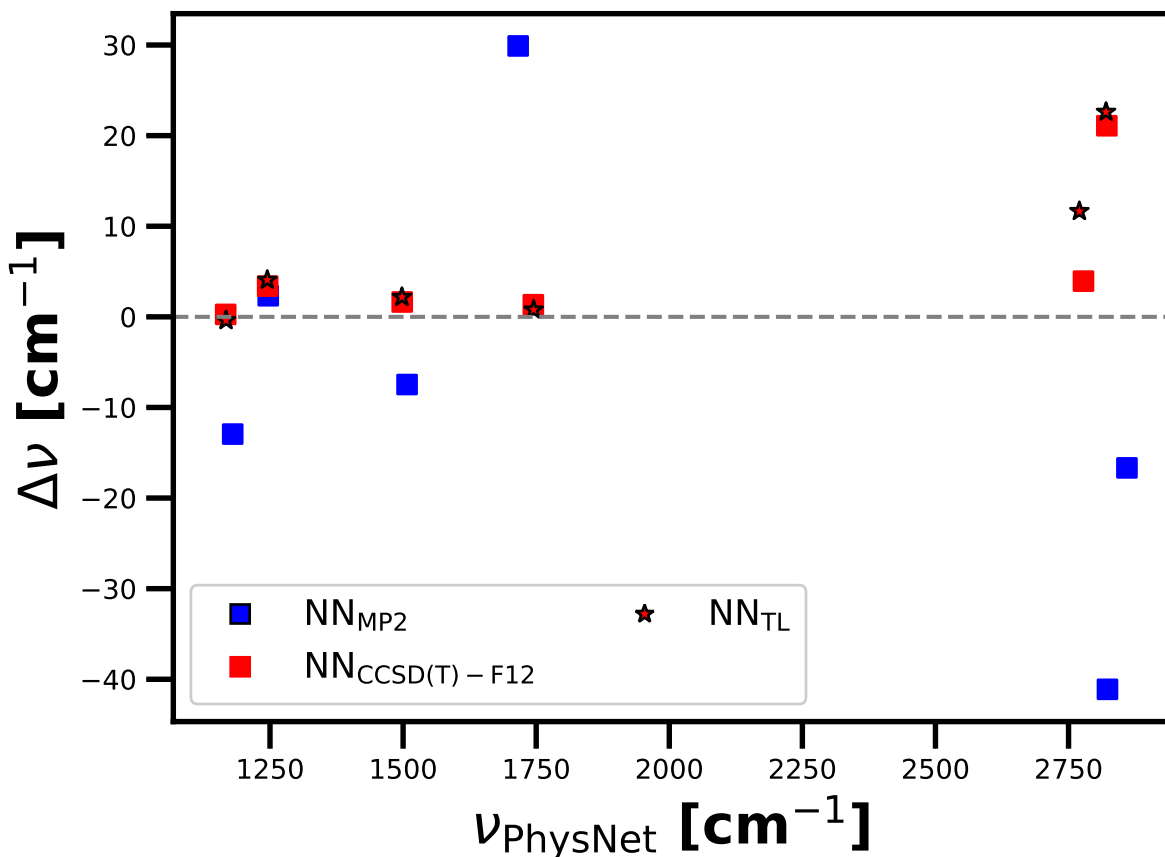


Figure 6: Comparison of VPT2 frequencies from PhysNet trained on MP2 ( $\text{NN}_{\text{MP2}}$ ), CCSD(T)-F12 ( $\text{NN}_{\text{CCSD(T)-F12}}$ ) and TL ( $\text{NN}_{\text{TL}}$ ) from MP2 to CCSD(T)-F12 with the experiment<sup>41</sup> for H<sub>2</sub>CO. Here,  $\Delta\nu = \nu_{\text{exp}} - \nu_{\text{PhysNet}}$ . The VPT2 frequencies on the TL-PES are within 8 cm<sup>-1</sup> to the values obtained from a model trained from scratch yielding an improvement in comparison to an MP2 model (its “starting point”).

els and might give less meaningful results statistically. The evaluation of the separate test set for all molecules yields MAEs( $E$ ) smaller than 0.03 kcal/mol and MAE( $F$ ) smaller than 0.02 kcal/mol/Å (compare to Figure 1 and 2) and are within the realm of what was expected. The MAEs and RMSEs of energies and forces for all TL models are listed in Table S28 for completeness.

A second measure of performance are the harmonic frequencies which can be compared with those from direct *ab initio* calculations. Even though optimizations and normal mode cal-

culations at the CCSD(T) level become computationally expensive rather quickly for larger molecules, they were performed for all the larger molecules  $\text{CH}_3\text{CHO}$ ,  $\text{CH}_3\text{NO}_2$ ,  $\text{CH}_3\text{COOH}$  and  $\text{CH}_3\text{CONH}_2$ . For  $\text{CH}_3\text{CHO}$ ,  $\text{CH}_3\text{NO}_2$  and  $\text{CH}_3\text{COOH}$  the harmonic frequencies on the TL PhysNet models compare to within  $\text{MAE}(\omega) = 0.2 \text{ cm}^{-1}$ ,  $\text{MAE}(\omega) = 0.3 \text{ cm}^{-1}$  and  $\text{MAE}(\omega) = 0.1 \text{ cm}^{-1}$  with the explicit calculations at the CCSD(T) level of theory, see Tables S29 to S31. These errors are also within those achieved by the models trained from scratch. Slightly larger errors are found for  $\text{CH}_3\text{CONH}_2$  ( $\text{MAE}(\omega) = 1.1 \text{ cm}^{-1}$ , see Table S32).

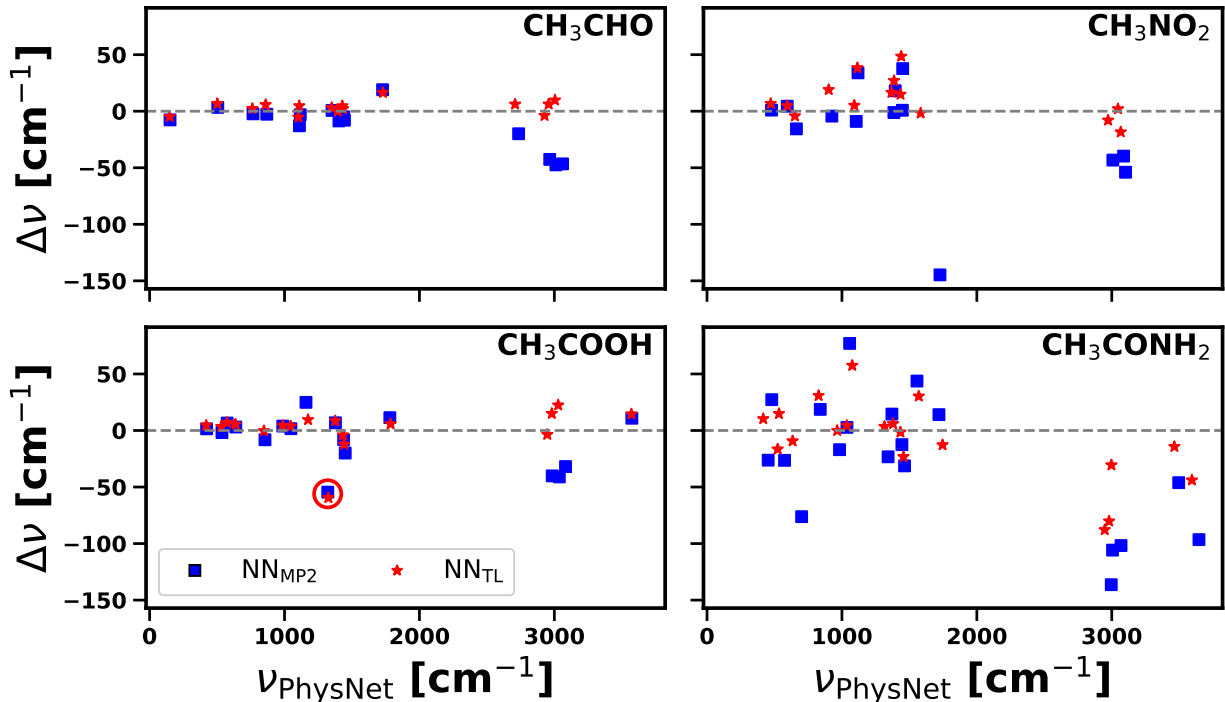


Figure 7: Comparison of the VPT2 frequencies from PhysNet trained on MP2 ( $\text{NN}_{\text{MP2}}$ , blue squares) and TL to CCSD(T) ( $\text{NN}_{\text{TL}}$ , red asterisks) with experimental values. Here,  $\Delta\nu = \nu_{\text{exp}} - \nu_{\text{PhysNet}}$ . The TL models yield overall improved VPT2 frequencies, especially for the high frequency modes. A rather large deviation is found for the frequency around  $1300 \text{ cm}^{-1}$  for  $\text{NN}_{\text{TL}}$  for  $\text{CH}_3\text{COOH}$ . A red circle marks a surprisingly high error, compared to the other modes. It is possible that this discrepancy is caused by a misassignment of experimental modes, see text.

Finally, the performance of the models transfer learned to CCSD(T) can be assessed by comparing the VPT2 frequencies with experiment, see Figure 7. As a reference, the VPT2

frequencies from PhysNet models trained on MP2 data (blue squares) are reported together with the TL models. It is apparent that the TL models are closer to experiment especially for the high frequency modes and all MAEs( $\nu$ ) with respect to experiment are reduced, see Table 1. For CH<sub>3</sub>CHO the MAE( $\nu$ ) is reduced from 15.3 to 5.5 cm<sup>-1</sup>, corresponding to a factor of almost 3, while for the remaining three molecules this factor is closer to 2. Good agreement is found for CH<sub>3</sub>CHO, CH<sub>3</sub>NO<sub>2</sub> and CH<sub>3</sub>COOH while the picture is less clear for CH<sub>3</sub>CONH<sub>2</sub>.

**Table 1: MAEs of the PhysNet VPT2 frequencies with respect to experimental values.<sup>41–48</sup> The level of theory of the training data is given in the header and the results of the transfer learned PhysNet models are highlighted in bold. An additional column shows the MAEs of the “conventional” approach where harmonic frequencies are scaled by an empirical factor<sup>57</sup> (see also Figure S1 for an illustration of the scaled frequencies compared with experiment).**

MAE( $\nu$ ) [cm <sup>-1</sup> ]	MP2	CCSD(T)	CCSD(T)-F12	scaled MP2/CCSD(T)
H <sub>2</sub> CO	18.40	9.04	3.98/ <b>6.95</b>	48.22/37.74
HONO	26.98	5.56	6.74	38.44/17.31
HCOOH	17.61	9.06	3.59	32.99/26.31
CH <sub>3</sub> OH	27.28	14.30	–	23.47/19.60
CH <sub>3</sub> CHO	15.27	<b>5.47</b>	–	29.04/21.90
CH <sub>3</sub> COOH	16.25	<b>10.83</b>	–	21.39/19.74
CH <sub>3</sub> NO <sub>2</sub>	28.56	<b>15.38</b>	–	34.27/25.28
CH <sub>3</sub> CONH <sub>2</sub>	47.23	<b>25.13</b>	–	43.46/34.81

### 3.5 Timings

By using *ab initio* calculations (see Table S1 for cost of *ab initio* energy, forces and dipole moment calculations) and a PhysNet representation of the underlying PES, it is possible to determine VPT2 frequencies at considerably higher levels of theory for larger molecules than is possible from straight *ab initio* evaluations. This raises the question: how do the computational efficiencies of the different approaches compare?

The following points are considered:

- *Feasibility at a given ab initio level:* VPT2 calculations at the MP2 level have been performed for all molecules considered. The calculation times ranged from few CPU hours for the small molecules ( $\text{H}_2\text{CO}$ : 2.5 h,  $\text{HONO}$ : 5 h), to multiple CPU hours for  $\text{HCOOH}/\text{CH}_3\text{OH}$  (14 h) and  $\text{CH}_3\text{CHO}$  (60 h) up to several days for the largest molecules ( $\text{CH}_3\text{COOH}$ : 190 h,  $\text{CH}_3\text{NO}_2$ : 103 h,  $\text{CH}_3\text{CONH}_2$ : 298 h). However, compared with experiment, VPT2 frequencies at the MP2 level of theory were found to be inferior to CCSD(T) with unsigned deviations of up to  $150\text{ cm}^{-1}$ , see Table 1. While a full CCSD(T) VPT2 treatment for the smallest molecules would be possible, this will be too costly for the larger structures. It was reported<sup>58</sup> that a VPT2 calculation for  $\text{H}_2\text{CO}$  at various levels of theory is around 10 times more expensive than the calculation of harmonic frequencies. This is also found in the present work. Even though this factor will increase for larger molecules (as more derivatives need to be evaluated) it can be used to tentatively assess the cost of a CCSD(T) VPT2 treatment of a larger molecule. The calculation of harmonic frequencies of  $\text{CH}_3\text{CONH}_2$  at the CCSD(T) level is found to take more than 20 CPU days which suggests that a CCSD(T) VPT2 calculation would take more than 200 CPU days.
- *Data Generation and Learning of PhysNet:* The time for generating a PhysNet model includes computation of a data set (*ab initio* calculations of energies, forces and dipole moments), training and validating the NN. The most costly steps are the training ( $\leq 5$  days) and, depending on the level of theory, the calculation of the reference data. As an example, generating the most expensive data set (5401  $\text{HCOOH}$  geometries at the CCSD(T)-F12 level:  $\sim 130$  CPU min per calculation) takes around two days assuming that 250 calculations can be performed in parallel (the “real time” of the calculations might be longer depending on I/O performance). The PhysNet VPT2 calculation then is the least expensive step, taking less than 1 hour ( $\text{H}_2\text{CO}$ : 18 min,



CH<sub>3</sub>CONH<sub>2</sub>: 58 min).

As an explicit example, data generation at the MP2 level, NN training and VPT2 calculations for CH<sub>3</sub>COOH or CH<sub>3</sub>CONH<sub>2</sub> are considered. With a conservative estimate for generating reference data, fitting and testing of the PhysNet model of 7 days, a direct *ab initio* VPT2 calculation at the MP2 level of theory exceeds the cost of the NN + VPT2 approach for these two molecules by a factor of 1.1 (10 %) and 1.7 (70 %), respectively. For larger molecules this factor increases further as it does also for higher-level methods. In addition, the approach pursued here has the added benefit of a full-dimensional, near-equilibrium PES that can also be used for MD simulations, albeit some additional reference calculations may be required.

- *Crossover between NN + VPT2 versus ab initio*: It is of interest to ask at what point does the NN + VPT2 approach become advantageous over the *ab initio* approach in terms of overall computational cost. For the higher levels of theory the cost of *ab initio* VPT2 calculations scales less favourably than single (energy, forces and dipole moment) calculations due to the repetitive evaluation of first- to fourth-order derivatives of the potential energy. If the cost for an *ab initio* VPT2 calculation is estimated<sup>58</sup> as  $10 * t_{\text{harm}}$  (where  $t_{\text{harm}}$  is the time to calculate harmonic frequencies), then a PhysNet model becomes more favourable already for HCOOH at the CCSD(T) level ( $t_{\text{harm}} = 30$  h). The preference of the NN + VPT2 approach for larger molecules and higher levels is even more apparent when using TL. As an example, the CCSD(T) data set for CH<sub>3</sub>CONH<sub>2</sub> (632 data points; the calculations including energy, forces and dipole moments take  $\sim 9$  CPU hours on average while the real time was closer to 15 h) is generated in less than 2 days, and the TL can be performed with costs on the order of 1 hour. Together with the time for reference data generation at the MP2 level, training and evaluating of the base NN, the total estimated time for VPT2 frequencies for CH<sub>3</sub>CONH<sub>2</sub> at

the CCSD(T) level on the order of 10 CPU days, compared with an estimated 200 CPU days from a brute force calculation. Empirically, this is close to linear scaling, whereas at the *ab initio* level the scaling increases formally from  $N^5$  for MP2 to  $N^7$  for CCSD(T).<sup>59</sup>

In summary, while at the MP2 level the NN + VPT2 approach is computationally superior only for the two largest molecules, it outperforms the *ab initio* approach at higher levels for all but tetra-atomic molecules. The feasibility of the NN + VPT2 approach for larger molecules and higher levels is strengthened when employing TL.

## 4 Discussion

The results presented so far have established that a ML model yields the same normal mode and VPT2 frequencies as direct evaluations from electronic structure calculations and comparison between computations and experiments is favourable (unsigned deviations between  $< 0.5$  and  $21 \text{ cm}^{-1}$  for the CCSD(T)-F12 models and between  $< 0.5$  and  $88 \text{ cm}^{-1}$  for the CCSD(T) models, including TL). Alternatively, calculated normal mode frequencies are often scaled by empirical factors to compare directly with experiment.<sup>60</sup> Table 1 summarizes the mean absolute errors between experimentally measured frequencies, those from VPT2 calculations at the three levels of theory, and the scaled harmonic frequencies from MP2 and CCSD(T) calculations (last column). Scaled MP2 and CCSD(T) frequencies differ on average by  $20 \text{ cm}^{-1}$  to  $50 \text{ cm}^{-1}$  from those measured experimentally. This is comparable to the difference between (anharmonic) VPT2 calculations at the MP2 level on the PhysNet-PES and experiment. On the other hand, VPT2 calculations on the CCSD(T) and CCSD(T)-F12 PESs are in better agreement (average MAE of  $10 \text{ cm}^{-1}$  and  $5 \text{ cm}^{-1}$ ) and clearly outperform results from MP2 calculations (scaled harmonic and VPT2) and scaled harmonic CCSD(T)

frequencies.

Application of TL showed that the harmonic frequencies of the TL models reach  $\text{MAE}(\omega)$  with respect to reference comparable to models trained from scratch. The small additional cost for obtaining a high-quality PES from a lower-level PES and the rapid scaling of the costs for obtaining *ab initio* harmonic frequencies motivates the use of TL for the determination of high quality harmonic frequencies for which fully-dimensional *ab initio* PESs are computationally too expensive.

Comparison of accurate (anharmonic) VPT2 frequencies with experiment can provide additional insight. Such comparisons depend on the quality of the computations and that of the experiment. One particularly appealing possibility is to compare and potentially reassign individual modes. As an example, the OH bending vibration of monomeric formic acid is considered. The early infrared studies were carried out in the late 1950s by Milliken and Pitzer<sup>49</sup> and by Miyazawa and Pitzer,<sup>61</sup> where the OH bending vibration was assigned to a signal at  $1229\text{ cm}^{-1}$ . Later work (see e.g. Refs. 62 or 63 and references therein) reported an OH bending frequency of  $1223\text{ cm}^{-1}$  consistent with the earlier work. An OH bending frequency of  $1223\text{ cm}^{-1}$  is  $\sim 80\text{ cm}^{-1}$  lower than what is found from VPT2 calculations on the PhysNet PES at the CCSD(T)-F12 level of theory which finds it at  $1302\text{ cm}^{-1}$ .

Recent theoretical work determined vibrational frequencies from vibrational configuration interaction (VCI) calculations on a global CCSD(T)(F12\*)/cc-pVTZ-F12 PES for cis- and trans-formic acid and tried to re-assign experimentally determined fundamental, overtone and combination bands.<sup>43,62</sup> These calculations proposed to assign the fundamental OH bend to an experimentally measured frequency at  $1306.2\text{ cm}^{-1}$  and the first overtone of the OH torsion to a frequency at  $1223\text{ cm}^{-1}$ , converse to previous assignments.<sup>62</sup> Due to the rather close spacing, these two vibrations are in strong 1:2 Fermi resonance. This assignment

(see Figure 5) is consistent with the VPT2 calculations on the PhysNet(CCSD(T)-F12) PES results which find the OH bend at  $1301.9 \text{ cm}^{-1}$ . In addition, the first overtone of the OH torsion can also be calculated using PhysNet + VPT2 and is found at  $1220.2 \text{ cm}^{-1}$ , only  $3 \text{ cm}^{-1}$  away from an experimentally determined signal. Given the agreement of the two recent high-level computational treatments, based on very different approaches, and the fact that experiment indeed finds vibrational bands around  $1220$  and  $1300 \text{ cm}^{-1}$ , a reassignment of the fundamental OH bend to a frequency of  $1306.2 \text{ cm}^{-1}$  is supported.

A similar situation arises for  $\text{CH}_3\text{COOH}$  (Figure 7, red circle), where the signal at  $1325.5 \text{ cm}^{-1}$  from VPT2 calculation on the TL PhysNet(CCSD(T)) PES disagrees by  $\sim 60 \text{ cm}^{-1}$  from the experimentally measured frequency at  $1266 \text{ cm}^{-1}$ .<sup>46</sup> While (mostly) older studies<sup>64-67</sup> assigned the C-O stretch to a frequency around  $1260 \text{ cm}^{-1}$  and the OH bend to a lower frequency around  $1180 \text{ cm}^{-1}$ , more recent work came to a converse assignment<sup>46,68</sup> ( $\nu_7 = 1266 \text{ cm}^{-1}$  and  $\nu_8 = 1184 \text{ cm}^{-1}$ , following the notation in Reference 46). Goubet et al.<sup>46</sup> noted that  $\nu_7$  and  $\nu_8$  are not well predicted by theoretical calculations at the anharmonic level (RI-MP2/aVQZ harmonic frequencies corrected with VPT2 corrections obtained at the B98/aVQZ level following  $\nu_{\text{RI-MP2}} = \omega_{\text{RI-MP2}} - (\omega_{B98} - \nu_{B98})$ ) and ascribed the discrepancy to Fermi resonances between  $\nu_7$  and  $\nu_8$  with the first overtone of  $\nu_{16}$  ( $A''$  fundamental at  $642 \text{ cm}^{-1}$ ) and  $\nu_{11}$  ( $A''$  fundamental at  $581.5 \text{ cm}^{-1}$ ). Similarly, a large deviation of  $-60 \text{ cm}^{-1}$  between TL PhysNet(CCSD(T)) and  $\nu_7$  is found in this study compared with  $-61 \text{ cm}^{-1}$  in Reference 46.

Besides Fermi resonance as an explanation for the discrepancies, little work has been done on overtone and combination bands. Reference 69, however, suggested an alternative assignment of two bands at  $1324.4$  and  $1259.4 \text{ cm}^{-1}$  previously observed in the IR spectra of acetic acid isolated in Ar matrix.<sup>66,70</sup> They proposed to reassign the frequency at  $1324.4 \text{ cm}^{-1}$  to  $\nu_7$  and  $1259.4 \text{ cm}^{-1}$  to the first overtone of  $\nu_{16}$  based on VPT2 calculations at the B3LYP/6-

311++G(2d,2p) level and deuteration experiments. This new assignment is supported by the NN + VPT2 results yielding frequencies of 1325.5 and 1250.2  $\text{cm}^{-1}$  for  $\nu_7$  and  $2\nu_{16}$ , respectively. These present findings, for formic acid and acetic acid, encourage further theoretical work on overtones and combination bands.

## 5 Conclusion and Outlook

The combined NN + VPT2 approach together with TL is shown to provide accurate anharmonic frequencies at high levels of electronic structure theory. The PhysNet code was adapted to additionally predict analytical derivatives of the dipole moment  $\boldsymbol{\mu}$  and second order derivatives of  $E$  with respect to Cartesian coordinates (i.e. Hessians). Because for many high-level electronic structure methods analytical second derivatives are not explicitly implemented, the present NN-based approach is advantageous both, in terms of accuracy and computational efficiency. The present method can be systematically improved by using data at higher levels of theory, explicitly or by using TL, and allows to obtain VPT2 frequencies at levels of theory for which *ab initio* VPT2 calculation are impractical.

The current study can be extended to include IR intensities for fundamentals, combination bands and overtones. Moreover, the approach can be extended to investigate larger molecules and assist in (re)assigning experimental IR spectra. It is also shown that for the smallest molecules and the lowest level of theory considered (MP2/aug-cc-pVTZ) direct evaluation of harmonic and VPT2 frequencies is computationally more efficient than the combined NN + VPT2 approach. However, for molecules with 6 and more atoms and for the higher levels of quantum chemical treatment (CCSD(T) and higher) the NN + VPT2 approach is computationally considerably more efficient. Finally, the VPT2 frequencies at these highest levels of theory compare favourably (to within a few  $\text{cm}^{-1}$ ) with experimentally determined

frequencies. One additional application for high-level VPT2 calculations is the accurate determination of dimerization energies, such as H-bonded complexes, for which accurate anharmonic zero point vibrational energies are required.<sup>71</sup> Also, using DFT calculations for the reference ML model in TL to higher levels of theory is an attractive prospect to further improve the efficiency of the present method. Finally, additional improvements may be achieved by using sophisticated sampling or learning approaches such as active learning.<sup>72</sup>

## Data Availability Statement

The PhysNet codes are available at <https://github.com/MMunibas/PhysNet>, and the VibML dataset containing the reference data can be downloaded from Zenodo <https://doi.org/10.5281/zenodo.117810>, <https://doi.org/10.5281/zenodo.200020>, <https://doi.org/10.5281/zenodo.188724> and the NCCR MUST, and the University of Basel.

## Acknowledgments

This work was supported by the Swiss National Science Foundation through grants 200021-117810, 200020-188724 and the NCCR MUST, and the University of Basel.

## References

- (1) Qu, C.; Bowman, J. M. Quantum approaches to vibrational dynamics and spectroscopy: is ease of interpretation sacrificed as rigor increases? *Phys. Chem. Chem. Phys.* **2019**, *21*, 3397–3413.
- (2) Unke, O. T.; Koner, D.; Patra, S.; Käser, S.; Meuwly, M. High-dimensional potential energy surfaces for molecular simulations: from empiricism to machine learning. *Mach.Learn.: Sci. Technol.* **2020**, *1*, 013001.
- (3) Käser, S.; Koner, D.; Christensen, A. S.; von Lilienfeld, O. A.; Meuwly, M. Machine

- Learning Models of Vibrating H<sub>2</sub>CO: Comparing Reproducing Kernels, FCHL, and PhysNet. *J. Phys. Chem. A* **2020**, *124*, 8853–8865.
- (4) Qu, C.; Conte, R.; Houston, P. L.; Bowman, J. M. Full-dimensional potential energy surface for acetylacetone and tunneling splittings. *Phys. Chem. Chem. Phys.* **2021**, <http://dx.doi.org/10.1039/D0CP04221H>.
- (5) Nejad, A.; Meyer, E.; Suhm, M. A. Glycolic Acid as a Vibrational Anharmonicity Benchmark. *J. Phys. Chem. Lett.* **2020**, *11*, 5228–5233.
- (6) Mata, R. A.; Suhm, M. A. Benchmarking quantum chemical methods: Are we heading in the right direction? *Angew. Chem. Int. Ed.* **2017**, *56*, 11011–11018.
- (7) Barone, V.; Biczysko, M.; Bloino, J. Fully anharmonic IR and Raman spectra of medium-size molecular systems: accuracy and interpretation. *Phys. Chem. Chem. Phys.* **2014**, *16*, 1759–1787.
- (8) Qu, C.; Bowman, J. M. IR Spectra of (HCOOH)<sub>2</sub> and (DCOOH)<sub>2</sub>: Experiment, VSCF/VCI, and Ab Initio Molecular Dynamics Calculations Using Full-Dimensional Potential and Dipole Moment Surfaces. *J. Phys. Chem. Lett.* **2018**, *9*, 2604–2610.
- (9) Qu, C.; Bowman, J. M. Quantum and classical IR spectra of (HCOOH)<sub>2</sub>,(DCOOH)<sub>2</sub> and (DCOOD)<sub>2</sub> using ab initio potential energy and dipole moment surfaces. *Faraday Discuss.* **2018**, *212*, 33–49.
- (10) Qu, C.; Bowman, J. M. High-dimensional fitting of sparse datasets of CCSD (T) electronic energies and MP2 dipole moments, illustrated for the formic acid dimer and its complex IR spectrum. *J. Chem. Phys.* **2018**, *148*, 241713.
- (11) Koner, D.; Meuwly, M. Permutationally invariant, reproducing kernel-based potential energy surfaces for polyatomic molecules: From formaldehyde to acetone. *J. Chem. Theory. Comput.* **2020**, *16*, 5474–5484.

- (12) Frisch, M. J.; Trucks, G. W.; Schlegel, H. B.; Scuseria, G. E.; Robb, M. A.; Cheeseman, J. R.; Scalmani, G.; Barone, V.; Mennucci, B.; Petersson, G. A. et al. Gaussian 09 Revision E.01. Gaussian Inc. Wallingford CT 2009.
- (13) Barone, V. Anharmonic vibrational properties by a fully automated second-order perturbative approach. *J. Chem. Phys.* **2005**, *122*, 014108.
- (14) Taylor, M. E.; Stone, P. Transfer learning for reinforcement learning domains: A survey. *J. Mach. Learn. Res.* **2009**, *10*, 1633–1685.
- (15) Pan, S. J.; Yang, Q. A survey on transfer learning. *IEEE Trans. Knowl. Data Eng.* **2009**, *22*, 1345–1359.
- (16) Møller, C.; Plesset, M. S. Note on an approximation treatment for many-electron systems. *Phys. Rev.* **1934**, *46*, 618–622.
- (17) Kendall, R. A.; Dunning Jr, T. H.; Harrison, R. J. Electron affinities of the first-row atoms revisited. Systematic basis sets and wave functions. *J. Chem. Phys.* **1992**, *96*, 6796–6806.
- (18) Pople, J. A.; Head-Gordon, M.; Raghavachari, K. Quadratic configuration interaction. A general technique for determining electron correlation energies. *J. Chem. Phys.* **1987**, *87*, 5968–5975.
- (19) Purvis III, G. D.; Bartlett, R. J. A full coupled-cluster singles and doubles model: The inclusion of disconnected triples. *J. Chem. Phys.* **1982**, *76*, 1910–1918.
- (20) Adler, T. B.; Knizia, G.; Werner, H.-J. A simple and efficient CCSD (T)-F12 approximation. *J. Chem. Phys.* **2007**, *127*, 221106.
- (21) Peterson, K. A.; Adler, T. B.; Werner, H.-J. Systematically convergent basis sets for explicitly correlated wavefunctions: The atoms H, He, B–Ne, and Al–Ar. *J. Chem. Phys.* **2008**, *128*, 084102.



- (22) Werner, H.-J.; Knowles, P. J.; Knizia, G.; Manby, F. R.; Schütz, M.; Celani, P.; Györffy, W.; Kats, D.; Korona, T.; Lindh, R. et al. MOLPRO, version 2019, a package of ab initio programs. 2019.
- (23) Smith, J. S.; Isayev, O.; Roitberg, A. E. ANI-1, A data set of 20 million calculated off-equilibrium conformations for organic molecules. *Sci. Data* **2017**, *4*, 170193.
- (24) Bannwarth, C.; Ehlert, S.; Grimme, S. GFN2-xTB—An accurate and broadly parametrized self-consistent tight-binding quantum chemical method with multipole electrostatics and density-dependent dispersion contributions. *J. Chem. Theory Comput.* **2019**, *15*, 1652–1671.
- (25) Unke, O. T.; Meuwly, M. PhysNet: A neural network for predicting energies, forces, dipole moments, and partial charges. *J. Chem. Theory Comput.* **2019**, *15*, 3678–3693.
- (26) Gilmer, J.; Schoenholz, S. S.; Riley, P. F.; Vinyals, O.; Dahl, G. E. Neural message passing for quantum chemistry. Proc. of the 34th Int. Conf. on Machine Learning—Volume 70. 2017; pp 1263–1272.
- (27) Rivero, U.; Unke, O. T.; Meuwly, M.; Willitsch, S. Reactive atomistic simulations of Diels-Alder reactions: The importance of molecular rotations. *J. Chem. Phys.* **2019**, *151*, 104301.
- (28) Brickel, S.; Das, A. K.; Unke, O. T.; Turan, H. T.; Meuwly, M. Reactive molecular dynamics for the  $[\text{Cl}-\text{CH}_3-\text{Br}]^-$  reaction in the gas phase and in solution: a comparative study using empirical and neural network force fields. *Electron. Struct.* **2019**, *1*, 024002.
- (29) Käser, S.; Unke, O. T.; Meuwly, M. Reactive dynamics and spectroscopy of hydrogen transfer from neural network-based reactive potential energy surfaces. *New J. Phys.* **2020**, *22*, 055002.

- (30) Käser, S.; Unke, O. T.; Meuwly, M. Isomerization and decomposition reactions of acetaldehyde relevant to atmospheric processes from dynamics simulations on neural network-based potential energy surfaces. *J. Chem. Phys.* **2020**, *152*, 214304.
- (31) Sweeny, B. C.; Pan, H.; Kassem, A.; Sawyer, J. C.; Ard, S. G.; Shuman, N. S.; Viggiano, A. A.; Brickel, S.; Unke, O. T.; Upadhyay, M. et al. Thermal activation of methane by  $\text{MgO}^+$ : temperature dependent kinetics, reactive molecular dynamics simulations and statistical modeling. *Phys. Chem. Chem. Phys.* **2020**, *22*, 8913–8923.
- (32) Grimme, S.; Antony, J.; Ehrlich, S.; Krieg, H. A consistent and accurate ab initio parametrization of density functional dispersion correction (DFT-D) for the 94 elements H-Pu. *J. Chem. Phys.* **2010**, *132*, 154104.
- (33) Baydin, A. G.; Pearlmutter, B. A.; Radul, A. A.; Siskind, J. M. Automatic differentiation in machine learning: a survey. *J. Mach. Learn. Res.* **2017**, *18*, 5595–5637.
- (34) Abadi, M.; Agarwal, A.; Barham, P.; Brevdo, E.; Chen, Z.; Citro, C.; Corrado, G. S.; Davis, A.; Dean, J.; Devin, M. et al. TensorFlow: Large-Scale Machine Learning on Heterogeneous Systems. 2015; <https://www.tensorflow.org/>, Software available from tensorflow.org.
- (35) Reddi, S. J.; Kale, S.; Kumar, S. On the convergence of adam and beyond. *arXiv preprint arXiv:1904.09237* **2019**,
- (36) Nielsen, H. H. The vibration-rotation energies of molecules. *Rev. Mod. Phys.* **1951**, *23*, 90–136.
- (37) Stanton, J. F.; Gauss, J.; Cheng, L.; Harding, M. E.; Matthews, D. A.; Szalay, P. G. CFOUR, Coupled-Cluster techniques for Computational Chemistry, a quantum-chemical program package. With contributions from A.A. Auer, R.J. Bartlett, U. Benedikt, C. Berger, D.E. Bernholdt, S. Blaschke, Y. J. Bomble, S. Burger, O. Christiansen, D. Datta, F. Engel, R. Faber, J. Greiner, M. Heckert, O. Heun, M. Hilgenberg,

C. Huber, T.-C. Jagau, D. Jonsson, J. Jusélius, T. Kirsch, K. Klein, G.M. KopperW.J. Lauderdale, F. Lipparini, T. Metzroth, L.A. Mück, D.P. O’Neill, T. Nottoli, D.R. Price, E. Prochnow, C. Puzzarini, K. Ruud, F. Schiffmann, W. Schwalbach, C. Simmons, S. Stopkowicz, A. Tajti, J. Vázquez, F. Wang, J.D. Watts and the integral packages MOLECULE (J. Almlöf and P.R. Taylor), PROPS (P.R. Taylor), ABACUS (T. Helgaker, H.J. Aa. Jensen, P. Jørgensen, and J. Olsen), and ECP routines by A. V. Mitin and C. van Wüllen. For the current version, see <http://www.cfour.de>.

- (38) Yu, Q.; Bowman, J. M. Vibrational second-order perturbation theory (VPT2) using local monomer normal modes. *Mol. Phys.* **2015**, *113*, 3964–3971.
- (39) Bloino, J.; Biczysko, M.; Barone, V. General perturbative approach for spectroscopy, thermodynamics, and kinetics: Methodological background and benchmark studies. *J. Chem. Theory Comput.* **2012**, *8*, 1015–1036.
- (40) Bloino, J. A VPT2 Route to Near-Infrared Spectroscopy: The Role of Mechanical and Electrical Anharmonicity. *J. Phys. Chem. A* **2015**, *119*, 5269–5287.
- (41) Herndon, S. C.; Nelson Jr, D. D.; Li, Y.; Zahniser, M. S. Determination of line strengths for selected transitions in the  $\nu_2$  band relative to the  $\nu_1$  and  $\nu_5$  bands of H<sub>2</sub>CO. *J. Quant. Spectrosc. Radiat. Transf.* **2005**, *90*, 207–216.
- (42) Guilmot, J.; Godefroid, M.; Herman, M. Rovibrational parameters for trans-nitrous acid. *J. Mol. Spectrosc.* **1993**, *160*, 387–400.
- (43) Tew, D. P.; Mizukami, W. Ab initio vibrational spectroscopy of cis- and trans-formic acid from a global potential energy surface. *J. Phys. Chem. A* **2016**, *120*, 9815–9828.
- (44) Serrallach, A.; Meyer, R.; Günthard, H. H. Methanol and deuterated species: infrared data, valence force field, rotamers, and conformation. *J. Mol. Spectrosc.* **1974**, *52*, 94–129.

- (45) Wiberg, K. B.; Thiel, Y.; Goodman, L.; Leszczynski, J. Acetaldehyde: Harmonic Frequencies, Force Field, and Infrared Intensities. *J. Phys. Chem.* **1995**, *99*, 13850–13864.
- (46) Goubet, M.; Soulard, P.; Pirali, O.; Asselin, P.; Réal, F.; Gruet, S.; Huet, T. R.; Roy, P.; Georges, R. Standard free energy of the equilibrium between the trans-monomer and the cyclic-dimer of acetic acid in the gas phase from infrared spectroscopy. *Phys. Chem. Chem. Phys.* **2015**, *17*, 7477–7488.
- (47) Wells, A.; Wilson Jr, E. B. Infra-Red and Raman Spectra of Polyatomic Molecules XIII. Nitromethane. *J. Chem. Phys.* **1941**, *9*, 314–318.
- (48) Ganeshsrinivas, E.; Sathyanarayana, D.; Machida, K.; Miwa, Y. Simulation of the infrared spectra of acetamide by an extended molecular mechanics method. *J. Mol. Struct.* **1996**, *361*, 217–227.
- (49) Millikan, R. C.; Pitzer, K. S. Infrared spectra and vibrational assignment of monomeric formic acid. *J. Chem. Phys.* **1957**, *27*, 1305–1308.
- (50) Smith, J. S.; Nebgen, B. T.; Zubatyuk, R.; Lubbers, N.; Devereux, C.; Barros, K.; Tretiak, S.; Isayev, O.; Roitberg, A. Outsmarting quantum chemistry through transfer learning. *Preprint at [https://chemrxiv.org/articles/Outsmarting\\_Quantum\\_Chemistry\\_Through\\_Transfer\\_Learning/6744440](https://chemrxiv.org/articles/Outsmarting_Quantum_Chemistry_Through_Transfer_Learning/6744440)* **2018**,
- (51) Ramakrishnan, R.; Dral, P.; Rupp, M.; von Lilienfeld, O. A. Big Data meets quantum chemistry approximations: The  $\Delta$ -machine learning approach. *J. Chem. Theory Comput.* **2015**, *11*, 2087–2096.
- (52) Batra, R.; Pilania, G.; Uberuaga, B. P.; Ramprasad, R. Multifidelity information fusion with machine learning: A case study of dopant formation energies in hafnia. *ACS Appl. Mater. Interfaces* **2019**, *11*, 24906–24918.

- (53) Nandi, A.; Qu, C.; Houston, P. L.; Conte, R.; Bowman, J. M.  $\Delta$ -machine learning for potential energy surfaces: A PIP approach to bring a DFT-based PES to CCSD (T) level of theory. *J. Chem. Phys.* **2021**, *154*, 051102.
- (54) Mezei, P. D.; von Lilienfeld, O. A. Noncovalent Quantum Machine Learning Corrections to Density Functionals. *J. Chem. Theory. Comput.* **2020**, *16*, 2647–2653.
- (55) Meuwly, M.; Hutson, J. M. Morphing ab initio potentials: A systematic study of Ne–HF. *J. Chem. Phys.* **1999**, *110*, 8338–8347.
- (56) Bowman, J. M.; Gazdy, B. A simple method to adjust potential energy surfaces: Application to HCO. *J. Chem. Phys.* **1991**, *94*, 816–817.
- (57) Johnson, R. D. III. Computational Chemistry Comparison and Benchmark Data Base. <https://cccbdb.nist.gov/vibscalex.asp>, Release 21.
- (58) Jacobsen, R. L.; Johnson III, R. D.; Irikura, K. K.; Kacker, R. N. Anharmonic vibrational frequency calculations are not worthwhile for small basis sets. *J. Chem. Theory Comput.* **2013**, *9*, 951–954.
- (59) Friesner, R. A. Ab initio quantum chemistry: Methodology and applications. *Proc. Natl. Acad. Sci.* **2005**, *102*, 6648–6653.
- (60) Scott, A. P.; Radom, L. Harmonic vibrational frequencies: an evaluation of Hartree-Fock, Møller-Plesset, quadratic configuration interaction, density functional theory, and semiempirical scale factors. *J. Phys. Chem.* **1996**, *100*, 16502–16513.
- (61) Miyazawa, T.; Pitzer, K. S. Internal Rotation and Infrared Spectra of Formic Acid Monomer and Normal Coordinate Treatment of Out-of-Plane Vibrations of Monomer, Dimer, and Polymer. *J. Chem. Phys.* **1959**, *30*, 1076–1086.
- (62) Freytes, M.; Hurtmans, D.; Kassi, S.; Liévin, J.; Vander Auwera, J.; Campargue, A.; Herman, M. Overtone spectroscopy of formic acid. *Chem Phys* **2002**, *283*, 47–61.

- (63) Reva, I.; Plokhotnichenko, A.; Radchenko, E.; Sheina, G.; Blagoi, Y. P. The IR spectrum of formic acid in an argon matrix. *Spectrochim. Acta A* **1994**, *50*, 1107–1111.
- (64) Wilmshurst, J. Infrared Investigation of Acetic Acid and Acetic Acid-d Vapors and a Vibrational Assignment for the Monomeric Acids. *J. Chem. Phys.* **1956**, *25*, 1171–1173.
- (65) Haurie, M.; Novak, A. Spectres de vibration des molécules CH<sub>3</sub>COOH, CH<sub>3</sub>COOD, CD<sub>3</sub>COOH et CD<sub>3</sub>COOD-II.—Spectres infrarouges et Raman des dimères. *J. Chim. Phys.* **1965**, *62*, 146–157.
- (66) Berney, C.; Redington, R.; Lin, K. Infrared Spectra of Matrix-Isolated Acetic Acid Monomers. *J. Phys. Chem.* **1970**, *53*, 1713–1721.
- (67) Maçôas, E. M.; Khriachtchev, L.; Pettersson, M.; Fausto, R.; Räsänen, M. Rotational isomerism in acetic acid: the first experimental observation of the high-energy conformer. *J. Am. Chem. Soc.* **2003**, *125*, 16188–16189.
- (68) Maréchal, Y. IR spectra of carboxylic acids in the gas phase: A quantitative reinvestigation. *J. Chem. Phys.* **1987**, *87*, 6344–6353.
- (69) Olbert-Majkut, A.; Ahokas, J.; Lundell, J.; Pettersson, M. Raman spectroscopy of acetic acid monomer and dimers isolated in solid argon. *J. Raman Spectrosc.* **2011**, *42*, 1670–1681.
- (70) Macoas, E. M.; Khriachtchev, L.; Fausto, R.; Räsänen, M. Photochemistry and vibrational spectroscopy of the trans and cis conformers of acetic acid in solid Ar. *J. Phys. Chem. A* **2004**, *108*, 3380–3389.
- (71) Kollipost, F.; Larsen, R. W.; Domanskaya, A. V.; Noerenberg, M.; Suhm, M. A. Communication: The highest frequency hydrogen bond vibration and an experimental value for the dissociation energy of formic acid dimer. *J. Chem. Phys.* **2012**, *136*.

- (72) Smith, J. S.; Nebgen, B.; Lubbers, N.; Isayev, O.; Roitberg, A. E. Less is more: Sampling chemical space with active learning. *J. Chem. Phys.* **2018**, *148*, 241733.

# Supporting information: MP2 Is Not Good Enough: Transfer Learning ML Models for Accurate VPT2 Frequencies

Silvan Käser, Eric Boittier, Meenu Upadhyay, and Markus Meuwly\*

*Department of Chemistry, University of Basel, Klingelbergstrasse 80 , CH-4056 Basel,  
Switzerland.*

E-mail: [m.meuwly@unibas.ch](mailto:m.meuwly@unibas.ch)



## 1 Data sets

Table S1: CPU timings for single processor jobs for the ab initio calculations using the given levels of theory for a single calculation of energy, gradients and dipole moments with tightened convergence criteria. For entries with ?? the calculation failed either due to memory or space issues. Note that for example a CCSD(T)-F12 calculation for CH<sub>3</sub>CHO needed about 350 GB of space. For molecules 1 to 3 the calculation on CCSD(T)-F12, for molecule 4 the calculations on CCSD(T) and for molecules 5 to 8 the calculations on the MP2 level of theory were performed. While the timing calculations were performed on a Intel(R) Xeon(R) CPU E5-2630 v4 @ 2.20GHz for consistency, the remaining calculations were performed on mixed computer architectures.

#	Molec	MP2/AVTZ	CCSD(T)/AVTZ	CCSD(T)-F12/AVTZ-F12
1	H <sub>2</sub> CO	0.5 min	5.5 min	18.5 min
2	HONO	1.0 min	27.0 min	88.0 min
3	HCOOH	1.5 min	33.5 min	130.0 min
4	CH <sub>3</sub> OH	1.0 min	21.5 min	70.0 min
5	CH <sub>3</sub> CHO	4.5 min	102.0 min	255.0 min
6	CH <sub>3</sub> NO <sub>2</sub>	5.5 min	268.0 min	876.0 min
7	CH <sub>3</sub> COOH	9.0 min	380.0 min	??
8	CH <sub>3</sub> CONH <sub>2</sub>	11.0 min	600.0 min	??

## 2 Results

### 2.1 Energy- and force-errors

MP2	H <sub>2</sub> CO		HONO		HCOOH		CH <sub>3</sub> OH		CH <sub>3</sub> CHO		CH <sub>3</sub> COOH		CH <sub>3</sub> NO <sub>2</sub>		CH <sub>3</sub> CONH <sub>2</sub>	
	NN <sub>1</sub>	NN <sub>2</sub>	NN <sub>1</sub>	NN <sub>2</sub>	NN <sub>1</sub>	NN <sub>2</sub>	NN <sub>1</sub>	NN <sub>2</sub>	NN <sub>1</sub>	NN <sub>2</sub>	NN <sub>1</sub>	NN <sub>2</sub>	NN <sub>1</sub>	NN <sub>2</sub>	NN <sub>1</sub>	NN <sub>2</sub>
EMAE:	7.19	1.26	1.92	2.47	20.42	10.43	7.90	2.93	1.36	15.13	10.35	21.05	8.48	12.26	21.83	22.30
ERMSE:	7.19	1.26	3.92	7.01	20.46	10.47	7.98	3.13	3.54	15.51	10.52	21.20	8.54	12.47	22.96	24.36
FMAE:	1.42	1.41	5.79	5.64	6.75	6.92	7.44	7.24	13.25	13.01	13.50	14.06	9.65	8.55	36.49	40.02
FRMSE:	3.66	3.44	23.32	27.01	29.83	18.33	27.02	29.08	53.37	47.07	38.41	43.00	73.22	67.00	106.02	128.84
1-R2:	5.4E-6	1.7E-7	1.0E-8	3.0E-8	1.4E-5	3.6E-6	6.0E-7	9.0E-8	3.0E-7	5.8E-6	2.3E-6	9.1E-6	2.4E-6	5.2E-6	3.2E-6	3.6E-6
<b>CCSD(T)</b>	NN <sub>1</sub>	NN <sub>2</sub>	NN <sub>1</sub>	NN <sub>2</sub>	NN <sub>1</sub>	NN <sub>2</sub>	NN <sub>1</sub>	NN <sub>2</sub>	NN <sub>1</sub>	NN <sub>2</sub>	NN <sub>1</sub>	NN <sub>2</sub>	NN <sub>1</sub>	NN <sub>2</sub>	NN <sub>1</sub>	NN <sub>2</sub>
EMAE:	0.47	1.21	1.56	2.36	21.90	0.63	8.67	5.04								
ERMSE:	0.49	1.22	4.71	5.54	21.91	0.87	8.74	5.15								
FMAE:	1.48	1.49	4.87	5.74	5.93	6.73	6.56	7.32								
FRMSE:	4.25	4.19	14.94	15.21	21.64	27.07	22.61	23.59								
1-R2:	3.0E-8	1.6E-7	2.0E-8	2.0E-8	1.6E-5	2.0E-8	7.5E-7	2.6E-7								
<b>CCSD(T)-F12</b>	NN <sub>1</sub>	NN <sub>2</sub>	NN <sub>1</sub>	NN <sub>2</sub>	NN <sub>1</sub>	NN <sub>2</sub>	NN <sub>1</sub>	NN <sub>2</sub>	NN <sub>1</sub>	NN <sub>2</sub>	NN <sub>1</sub>	NN <sub>2</sub>	NN <sub>1</sub>	NN <sub>2</sub>	NN <sub>1</sub>	NN <sub>2</sub>
EMAE:	0.90	2.44	6.96	5.90	3.13	7.60										
ERMSE:	1.00	2.49	11.27	6.81	3.25	7.68										
FMAE:	2.02	2.43	5.09	5.15	6.24	5.69										
FRMSE:	5.13	6.44	15.97	17.34	26.35	23.51										
1-R2:	1.1E-7	6.7E-7	9.0E-8	3.0E-8	3.5E-7	2.0E-6										

**Table S2:** Performance measures of two PhysNet models trained independently on the same *ab initio* data and evaluated on the test set. The MAEs and RMSEs are given in kcal/mol(/Å) and multiplied by a factor of 1000 for clarity.

## 2.2 H<sub>2</sub>CO

**Table S3:** Normal mode frequencies (in cm<sup>-1</sup>) of H<sub>2</sub>CO calculated from PhysNet models trained on MP2 data and compared to their reference *ab initio* values. The MAEs of the PhysNet predictions with respect to reference are given.

Mode	NN1(MP2)	NN2(MP2)	MP2	\Delta1	\Delta2
1	1196.65	1196.65	1196.70	0.05	0.05
2	1266.71	1266.70	1266.64	0.07	0.06
3	1539.99	1539.91	1539.91	0.08	0.00
4	1752.61	1752.47	1752.51	0.10	0.04
5	2973.23	2973.11	2973.27	0.04	0.16
6	3047.04	3047.10	3047.30	0.26	0.20
<b>MAE:</b>	0.10	0.09			

**Table S4:** Normal mode frequencies (in cm<sup>-1</sup>) of H<sub>2</sub>CO calculated from PhysNet models trained on CCSD(T) data and compared to their reference *ab initio* values. The MAEs of the PhysNet predictions with respect to reference are given.

Mode	NN1(CCSD(T))	NN2(CCSD(T))	CCSD(T)	\Delta1	\Delta2
1	1181.00	1181.02	1181.05	0.05	0.03
2	1261.67	1261.64	1261.53	0.14	0.11
3	1529.54	1529.43	1529.42	0.12	0.01
4	1764.82	1764.73	1764.87	0.05	0.14
5	2932.10	2931.96	2932.13	0.03	0.17
6	2999.94	2999.79	3000.07	0.13	0.28
<b>MAE:</b>	0.09	0.13			

**Table S5:** Normal mode frequencies (in  $\text{cm}^{-1}$ ) of  $\text{H}_2\text{CO}$  calculated from PhysNet models trained on CCSD(T)-F12 data and compared to their reference *ab initio* values. The MAEs of the PhysNet predictions with respect to reference are given.

Mode	NN1(CCSD(T)-F12)	NN2(CCSD(T)-F12)	CCSD(T)-F12	$ \Delta 1 $	$ \Delta 2 $
1	1186.52	1186.50	1186.53	0.01	0.03
2	1268.15	1268.17	1268.08	0.07	0.09
3	1532.76	1532.72	1532.67	0.09	0.05
4	1776.40	1776.43	1776.53	0.13	0.10
5	2933.37	2933.57	2933.75	0.38	0.18
6	3005.45	3005.69	3005.75	0.30	0.06
<b>MAE:</b>	0.17	0.08			

Mode	NN1(MP2)	NN1(MP2)	MP2	NN1(CCSD(T))	NN1(CCSD(T))	NN1(CCSD(T)-F12)	NN1(CCSD(T)-F12)	Exp
1	1180.04	1179.94	1180.23	1163.73	1163.52	1166.36	1166.73	1167.00
2	1246.72	1246.67	1246.71	1240.62	1241.36	1246.01	1245.61	1249.00
3	1507.55	1507.47	1507.95	1493.89	1494.91	1498.43	1498.36	1500.00
4	1719.02	1716.10	1720.94	1729.94	1731.88	1745.32	1744.66	1746.00
5	2823.82	2823.11	2826.67	2775.38	2779.58	2783.01	2778.06	2782.00
6	2862.29	2859.67	2862.61	2819.51	2821.49	2825.99	2821.91	2843.00
MAE:	18.49	18.40		10.65	9.04	3.98	5.28	

**Table S6:** VPT2 anharmonic frequencies (in  $\text{cm}^{-1}$ ) of  $\text{H}_2\text{CO}$  calculated using PhysNet (NN1 and NN2) trained on MP2, CCSD(T) and CCSD(T)-F12 data. They are compared to their reference *ab initio* values (MP2) as well as with experiment.<sup>1</sup> The MP2 frequencies are added as the VPT2 calculation is feasible in Gaussian. The MAEs are given with respect to experiment.

## 2.3 HONO

**Table S7:** Normal mode frequencies (in  $\text{cm}^{-1}$ ) of HONO calculated from PhysNet models trained on MP2 data and compared to their reference *ab initio* values. The MAEs of the PhysNet predictions with respect to reference are given.

Mode	NN1(MP2)	NN2(MP2)	MP2	$ \Delta 1 $	$ \Delta 2 $
1	586.44	586.45	586.53	0.09	0.08
2	602.45	602.40	602.38	0.07	0.02
3	805.28	805.18	805.20	0.08	0.02
4	1283.39	1283.37	1283.28	0.11	0.09
5	1659.77	1659.76	1659.81	0.04	0.05
6	3754.55	3754.40	3754.95	0.40	0.55
<b>MAE:</b>	0.13	0.13			

**Table S8:** Normal mode frequencies (in  $\text{cm}^{-1}$ ) of HONO calculated from PhysNet models trained on CCSD(T) data and compared to their reference *ab initio* values. The MAEs of the PhysNet predictions with respect to reference are given.

Mode	NN1(CCSD(T))	NN2(CCSD(T))	CCSD(T)	$ \Delta 1 $	$ \Delta 2 $
1	565.06	565.02	564.84	0.22	0.18
2	617.31	617.34	617.20	0.11	0.14
3	815.84	815.85	815.79	0.05	0.06
4	1305.94	1305.95	1305.94	0.00	0.01
5	1715.12	1715.15	1715.35	0.23	0.20
6	3759.58	3759.68	3760.30	0.72	0.62
<b>MAE:</b>	0.22	0.20			

**Table S9: Normal mode frequencies (in  $\text{cm}^{-1}$ ) of HONO calculated from PhysNet models trained on CCSD(T)-F12 data and compared to their reference *ab initio* values. The MAEs of the PhysNet predictions with respect to reference are given.**

Mode	NN1(CCSD(T)-F12)	NN2(CCSD(T)-F12)	CCSD(T)-F12	$ \Delta 1 $	$ \Delta 2 $
1	573.12	573.07	573.02	0.10	0.05
2	631.54	631.55	631.40	0.14	0.15
3	831.14	831.23	831.14	0.00	0.09
4	1315.91	1315.85	1315.76	0.15	0.09
5	1733.36	1733.39	1733.55	0.19	0.16
6	3774.84	3774.96	3775.54	0.70	0.58
<b>MAE:</b>	0.21	0.19			

Mode	NN1(MP2)	NN1(MP2)	MP2	NN1(CCSD(T))	NN1(CCSD(T))	NN1(CCSD(T)-F12)	NN1(CCSD(T)-F12)	Exp
1	551.59	551.72	551.35	533.67	533.93	541.10	542.37	543.88
2	566.02	566.12	565.97	595.98	596.32	608.55	608.92	595.62
3	766.25	765.86	765.83	785.91	786.93	799.70	799.04	790.12
4	1235.12	1230.53	1233.45	1260.08	1260.91	1267.74	1267.88	1263.21
5	1637.07	1636.84	1637.31	1691.60	1691.48	1709.88	1710.24	1699.76
6	3580.86	3581.00	3577.17	3580.01	3581.84	3590.28	3586.80	3590.77
MAE:	26.98	27.83		6.14	5.56	6.74	7.14	

**Table S10:** VPT2 anharmonic frequencies (in  $\text{cm}^{-1}$ ) of HONO calculated using PhysNet (NN1 and NN2) trained on MP2, CCSD(T) and CCSD(T)-F12 data. They are compared to their reference *ab initio* values (MP2) as well as with experiment.<sup>2</sup> The MP2 frequencies are added as the VPT2 calculation is feasible in Gaussian. The MAEs are given with respect to experiment.



## 2.4 HCOOH

**Table S11:** Normal mode frequencies (in  $\text{cm}^{-1}$ ) of HCOOH calculated from PhysNet models trained on MP2 data and compared to their reference *ab initio* values. The MAEs of the PhysNet predictions with respect to reference are given.

Mode	NN1(MP2)	NN2(MP2)	MP2	$ \Delta 1 $	$ \Delta 2 $
1	625.93	625.97	625.86	0.07	0.11
2	675.16	675.14	675.28	0.12	0.14
3	1058.72	1058.68	1058.77	0.05	0.09
4	1130.58	1130.91	1130.60	0.02	0.31
5	1301.64	1301.70	1301.56	0.08	0.14
6	1409.12	1409.07	1408.91	0.21	0.16
7	1793.39	1793.17	1793.29	0.10	0.12
8	3123.89	3123.92	3123.94	0.05	0.02
9	3740.49	3740.31	3740.56	0.07	0.25
<b>MAE:</b>	0.08	0.15			

**Table S12:** Normal mode frequencies (in  $\text{cm}^{-1}$ ) of HCOOH calculated from PhysNet models trained on CCSD(T) data and compared to their reference *ab initio* values. The MAEs of the PhysNet predictions with respect to reference are given.

Mode	NN1(CCSD(T))	NN2(CCSD(T))	CCSD(T)	$ \Delta 1 $	$ \Delta 2 $
1	626.52	626.68	626.46	0.06	0.22
2	664.46	664.43	664.94	0.48	0.51
3	1050.94	1050.93	1050.99	0.05	0.06
4	1131.48	1131.52	1131.27	0.21	0.25
5	1310.97	1311.12	1310.78	0.19	0.34
6	1404.92	1404.91	1404.71	0.21	0.20
7	1802.52	1802.56	1802.63	0.11	0.07
8	3088.01	3087.86	3087.61	0.40	0.25
9	3741.66	3741.54	3741.84	0.18	0.30
<b>MAE:</b>	0.21	0.24			

**Table S13:** Normal mode frequencies (in  $\text{cm}^{-1}$ ) of HCOOH calculated from PhysNet models trained on CCSD(T)-F12 data and compared to their reference *ab initio* values. The MAEs of the PhysNet predictions with respect to reference are given.

Mode	NN1(CCSD(T)-F12)	NN2(CCSD(T)-F12)	CCSD(T)-F12	$ \Delta 1 $	$ \Delta 2 $
1	630.68	630.66	630.56	0.12	0.10
2	672.06	672.06	672.14	0.08	0.08
3	1055.17	1055.17	1055.23	0.06	0.06
4	1136.51	1136.47	1136.26	0.25	0.21
5	1315.68	1315.68	1315.48	0.20	0.20
6	1407.20	1407.08	1406.99	0.21	0.09
7	1811.85	1811.79	1811.81	0.04	0.02
8	3092.10	3091.79	3091.90	0.20	0.11
9	3755.50	3755.53	3755.69	0.19	0.16
<b>MAE:</b>	0.15	0.11			

Mode	NN1(MP2)	NN1(MP2)	MP2	NN1(CCSD(T))	NN1(CCSD(T))	NN1(CCSD(T)-F12)	NN1(CCSD(T)-F12)	Exp
1	619.28	618.68	619.54	620.37	619.30	626.05	625.78	626.16
2	642.69	641.62	641.78	630.86	630.52	637.65	637.58	640.72
3	1037.06	1036.44	1036.38	1028.34	1028.38	1033.08	1033.04	1033.47
4	1097.01	1096.67	1098.18	1099.54	1098.65	1104.11	1104.70	1104.85
5	1220.49	1219.25	1220.63	1294.92	1293.36	1301.99	1301.89	1306.20
6	1380.81	1380.24	1380.94	1375.30	1374.86	1377.35	1378.23	1380.00
7	1758.17	1757.89	1760.53	1765.98	1768.89	1774.44	1774.60	1776.83
8	2959.50	2960.15	2967.80	2923.05	2922.24	2924.61	2927.30	2942.00
9	3554.88	3555.83	3554.90	3557.15	3562.98	3565.70	3565.34	3570.50
<b>MAE:</b>	17.62	17.61		9.47	9.06	3.97	3.59	

**Table S14:** VPT2 anharmonic frequencies (in  $\text{cm}^{-1}$ ) of HCOOH calculated using PhysNet (NN1 and NN2) trained on MP2, CCSD(T) and CCSD(T)-F12 data. They are compared to their reference *ab initio* values (MP2) as well as with experiment.<sup>3</sup> The MP2 frequencies are added as the VPT2 calculation is feasible in Gaussian. The MAEs are given with respect to experiment.

## 2.5 CH<sub>3</sub>OH

Table S15: Normal mode frequencies (in cm<sup>-1</sup>) of CH<sub>3</sub>OH calculated from PhysNet models trained on MP2 data and compared to their reference *ab initio* values. The MAEs of the PhysNet predictions with respect to reference are given.

Mode	NN1(MP2)	NN2(MP2)	MP2	\Delta1	\Delta2
1	289.86	289.85	289.38	0.48	0.47
2	1056.62	1056.61	1056.64	0.02	0.03
3	1088.65	1088.59	1088.63	0.02	0.04
4	1183.93	1183.91	1183.87	0.06	0.04
5	1371.59	1371.60	1371.57	0.02	0.03
6	1491.97	1491.96	1492.01	0.04	0.05
7	1525.40	1525.42	1525.41	0.01	0.01
8	1535.71	1535.79	1535.80	0.09	0.01
9	3053.97	3054.05	3053.94	0.03	0.11
10	3125.24	3125.24	3125.08	0.16	0.16
11	3182.86	3182.88	3182.91	0.05	0.03
12	3859.73	3859.80	3859.62	0.11	0.18
<b>MAE:</b>	0.09	0.10			

**Table S16:** Normal mode frequencies (in  $\text{cm}^{-1}$ ) of  $\text{CH}_3\text{OH}$  calculated from PhysNet models trained on CCSD(T) data and compared to their reference *ab initio* values. The MAEs of the PhysNet predictions with respect to reference are given.

Mode	NN1(CCSD(T))	NN2(CCSD(T))	CCSD(T)	$ \Delta 1 $	$ \Delta 2 $
1	286.35	286.33	285.95	0.40	0.38
2	1053.43	1053.41	1053.38	0.05	0.03
3	1082.20	1082.18	1082.11	0.09	0.07
4	1175.88	1175.85	1175.72	0.16	0.13
5	1379.10	1379.11	1379.01	0.09	0.10
6	1483.92	1483.91	1483.86	0.06	0.05
7	1512.18	1512.20	1512.16	0.02	0.04
8	1522.63	1522.65	1522.67	0.04	0.02
9	3010.68	3010.64	3010.43	0.25	0.21
10	3068.92	3068.88	3068.65	0.27	0.23
11	3128.02	3127.96	3127.97	0.05	0.01
12	3843.44	3843.41	3843.27	0.17	0.14
<b>MAE:</b>	0.14	0.12			

Table S17: VPT2 anharmonic frequencies (in  $\text{cm}^{-1}$ ) of  $\text{CH}_3\text{OH}$  calculated using PhysNet (NN1 and NN2) trained on MP2 and CCSD(T) data. They are compared to their reference *ab initio* values (MP2) as well as with experiment.<sup>4</sup> The MP2 frequencies are added as the VPT2 calculation is feasible in Gaussian. The MAEs are given with respect to experiment. Note that the lowest experimental frequency was obtained from Ar-matrix measurements.

Mode	NN1(MP2)	NN1(MP2)	MP2	NN1(CCSD(T))	NN1(CCSD(T))	Exp
1	240.84	241.49	240.64	236.97	238.08	271.50
2	1031.16	1030.51	1030.29	1026.41	1027.04	1033.50
3	1069.23	1069.65	1069.25	1063.32	1063.78	1074.50
4	1154.53	1154.90	1155.02	1145.68	1145.95	1145.00
5	1321.89	1321.99	1321.98	1321.31	1322.05	1332.00
6	1457.42	1457.78	1457.30	1447.89	1448.52	1454.50
7	1483.39	1483.11	1483.22	1469.21	1468.55	1465.00
8	1490.11	1489.77	1489.48	1475.75	1475.62	1479.50
9	2998.34	2997.26	2996.01	2827.05	2829.22	2844.20
10	3000.01	3001.00	2996.40	2911.42	2912.12	2970.00
11	3048.63	3048.07	3046.42	2987.57	2988.73	2999.00
12	3688.76	3686.33	3687.39	3666.53	3667.99	3681.50
<b>MAE:</b>	27.57	27.28		15.07	14.30	

## 2.6 CH<sub>3</sub>CHO

Table S18: Normal mode frequencies (in cm<sup>-1</sup>) of CH<sub>3</sub>CHO calculated from PhysNet models trained on MP2 data and compared to their reference *ab initio* values. The MAEs of the PhysNet predictions with respect to reference are given.

Mode	NN1(MP2)	NN2(MP2)	MP2	\Delta1	\Delta2
1	160.92	160.91	160.54	0.38	0.37
2	506.62	506.67	506.58	0.04	0.09
3	779.28	779.25	779.24	0.04	0.01
4	905.34	905.34	905.34	0.00	0.00
5	1136.34	1136.34	1136.37	0.03	0.03
6	1143.70	1143.72	1143.64	0.06	0.08
7	1390.46	1390.48	1390.38	0.08	0.10
8	1426.61	1426.58	1426.75	0.14	0.17
9	1481.35	1481.32	1481.20	0.15	0.12
10	1493.68	1493.73	1493.54	0.14	0.19
11	1763.36	1763.45	1763.86	0.50	0.41
12	2955.29	2955.30	2954.41	0.88	0.89
13	3069.58	3069.48	3069.68	0.10	0.20
14	3149.19	3149.18	3149.53	0.34	0.35
15	3199.78	3199.83	3199.44	0.34	0.39
<b>MAE:</b>	0.22	0.23			

**Table S19:** VPT2 anharmonic frequencies (in  $\text{cm}^{-1}$ ) of  $\text{CH}_3\text{CHO}$  calculated using PhysNet (NN1 and NN2) trained on MP2 data. They are compared to their reference *ab initio* values (MP2) as well as with experiment.<sup>5</sup> The MP2 frequencies are added as the VPT2 calculation is feasible in Gaussian. The MAEs are given with respect to experiment.

Mode	NN1(MP2)	NN1(MP2)	MP2	Exp
1	150.37	151.46	149.94	143.80
2	505.60	505.45	505.96	508.80
3	766.03	766.42	765.11	764.10
4	867.46	868.57	867.05	865.90
5	1110.82	1110.70	1109.98	1097.80
6	1115.91	1116.88	1116.41	1113.80
7	1352.20	1351.93	1351.80	1352.60
8	1403.31	1403.48	1403.23	1394.90
9	1437.73	1438.49	1437.76	1433.50
10	1445.30	1444.24	1445.08	1436.30
11	1728.74	1726.97	1726.61	1746.00
12	2735.11	2735.32	2735.51	2715.40
13	2966.08	2965.81	2964.93	2923.20
14	3012.46	3011.77	3012.12	2964.30
15	3064.91	3060.87	3059.86	3014.30
<b>MAE:</b>	15.27	15.32		



## 2.7 CH<sub>3</sub>COOH

Table S20: Normal mode frequencies (in cm<sup>-1</sup>) of CH<sub>3</sub>COOH calculated from PhysNet models trained on MP2 data and compared to their reference *ab initio* values. The MAEs of the PhysNet predictions with respect to reference are given.

Mode	NN1(MP2)	NN2(MP2)	MP2	\Delta1	\Delta2
1	77.46	77.49	77.20	0.26	0.29
2	422.71	422.66	422.69	0.02	0.03
3	549.67	549.67	549.71	0.04	0.04
4	583.21	583.18	583.15	0.06	0.03
5	661.91	661.90	662.07	0.16	0.17
6	873.85	873.76	873.74	0.11	0.02
7	1008.24	1008.20	1008.18	0.06	0.02
8	1075.99	1075.94	1075.86	0.13	0.08
9	1206.09	1205.93	1205.89	0.20	0.04
10	1342.18	1342.04	1342.07	0.11	0.03
11	1422.08	1421.89	1421.91	0.17	0.02
12	1492.58	1492.45	1492.36	0.22	0.09
13	1501.13	1500.97	1500.98	0.15	0.01
14	1809.90	1809.91	1810.19	0.29	0.28
15	3097.30	3097.21	3097.34	0.04	0.13
16	3180.81	3180.82	3181.01	0.20	0.19
17	3223.21	3223.25	3223.17	0.04	0.08
18	3751.61	3751.59	3751.57	0.04	0.02
<b>MAE:</b>	0.13	0.09			

Table S21: VPT2 anharmonic frequencies (in  $\text{cm}^{-1}$ ) of  $\text{CH}_3\text{COOH}$  calculated using PhysNet (NN1 and NN2) trained on MP2 data. They are compared to their reference *ab initio* values (MP2) as well as with experiment.<sup>6</sup> The MP2 frequencies are added as the VPT2 calculation is feasible in Gaussian. The MAEs are given with respect to experiment. The lowest frequency was not reported in Ref. 6.

Mode	NN1(MP2)	NN1(MP2)	MP2	Exp
1	74.53	73.11	77.93	–
2	422.52	423.21	422.94	424.00
3	536.36	538.21	536.39	534.50
4	574.91	575.17	575.61	581.50
5	638.93	641.25	639.50	642.00
6	855.20	855.37	855.10	847.00
7	987.08	987.15	987.46	991.00
8	1047.38	1045.69	1047.31	1049.00
9	1159.13	1161.15	1159.17	1184.00
10	1320.53	1322.89	1320.83	1266.00
11	1377.70	1378.64	1378.53	1384.50
12	1438.15	1437.89	1439.69	1430.00
13	1449.95	1450.01	1450.29	1430.00
14	1780.63	1787.68	1780.90	1792.00
15	2984.12	2989.62	2989.40	2944.00
16	3037.04	3040.77	3040.41	2996.00
17	3082.90	3080.65	3080.19	3051.00
18	3574.65	3567.07	3568.62	3585.50
<b>MAE:</b>	16.25	16.67		

## 2.8 CH<sub>3</sub>NO<sub>2</sub>

**Table S22:** Normal mode frequencies (in cm<sup>-1</sup>) of CH<sub>3</sub>NO<sub>2</sub> calculated from PhysNet models trained on MP2 data and compared to their reference *ab initio* values. The MAEs of the PhysNet predictions with respect to reference are given.

Mode	NN1(MP2)	NN2(MP2)	MP2	\Delta1	\Delta2
1	27.68	27.54	28.91	1.23	1.37
2	478.64	478.70	478.65	0.01	0.05
3	610.36	610.29	610.43	0.07	0.14
4	669.74	669.73	669.67	0.07	0.06
5	940.48	940.47	940.48	0.00	0.01
6	1127.26	1127.31	1127.28	0.02	0.03
7	1148.84	1148.94	1148.99	0.15	0.05
8	1411.99	1411.96	1412.12	0.13	0.16
9	1430.56	1430.56	1430.54	0.02	0.02
10	1491.99	1492.04	1491.90	0.09	0.14
11	1502.66	1502.71	1502.67	0.01	0.04
12	1745.37	1745.15	1745.72	0.35	0.57
13	3115.32	3115.35	3115.24	0.08	0.11
14	3221.42	3221.49	3221.29	0.13	0.20
15	3247.85	3247.85	3247.61	0.24	0.24
<b>MAE:</b>	0.17	0.21			

**Table S23:** VPT2 anharmonic frequencies (in  $\text{cm}^{-1}$ ) of  $\text{CH}_3\text{NO}_2$  calculated using PhysNet (NN1 and NN2) trained on MP2 data. They are compared to their reference *ab initio* values (MP2) as well as with experiment.<sup>7</sup> The MP2 frequencies are added as the VPT2 calculation is feasible in Gaussian. The MAEs are given with respect to experiment. The lowest frequency was not reported in Ref. 7 and was negative in the VPT2 calculation.

Mode	NN1(MP2)	NN1(MP2)	MP2	Exp
1	-84.94	-55.88	-47.12	–
2	479.22	478.01	477.77	479.00
3	593.12	594.60	593.54	599.00
4	661.89	662.60	663.10	647.00
5	922.30	925.33	923.87	921.00
6	1104.10	1106.03	1105.09	1097.00
7	1120.33	1119.07	1119.84	1153.00
8	1385.86	1385.15	1385.96	1384.00
9	1394.18	1394.87	1395.09	1413.00
10	1447.35	1448.15	1448.14	1449.00
11	1448.21	1450.30	1449.79	1488.00
12	1713.45	1726.72	1727.56	1582.00
13	3011.56	3008.23	3006.22	2965.00
14	3086.54	3087.68	3086.01	3048.00
15	3107.14	3101.98	3106.89	3048.00
<b>MAE:</b>	28.56	29.12		

## 2.9 CH<sub>3</sub>CONH<sub>2</sub>

Table S24: Normal mode frequencies (in cm<sup>-1</sup>) of CH<sub>3</sub>CONH<sub>2</sub> calculated from PhysNet models trained on MP2 data and compared to their reference *ab initio* values. The MAEs of the PhysNet predictions with respect to reference are given.

Mode	NN1(MP2)	NN2(MP2)	MP2	$\Delta 1$	$\Delta 2$
1	33.70	31.89	33.19	0.51	1.30
2	137.63	134.99	139.64	2.01	4.65
3	427.85	428.12	427.97	0.12	0.15
4	521.86	522.31	522.32	0.46	0.01
5	547.79	547.63	547.83	0.04	0.20
6	659.90	660.50	660.40	0.50	0.10
7	861.13	861.06	861.05	0.08	0.01
8	989.55	989.63	989.39	0.16	0.24
9	1060.85	1060.61	1060.44	0.41	0.17
10	1119.95	1119.96	1119.90	0.05	0.06
11	1353.38	1353.30	1353.21	0.17	0.09
12	1412.89	1412.92	1412.90	0.01	0.02
13	1492.30	1492.32	1492.32	0.02	0.00
14	1510.95	1510.80	1510.96	0.01	0.16
15	1623.80	1624.11	1623.89	0.09	0.22
16	1765.77	1765.60	1765.94	0.17	0.34
17	3086.67	3086.85	3086.75	0.08	0.10
18	3174.52	3174.68	3174.53	0.01	0.15
19	3198.69	3198.06	3198.43	0.26	0.37
20	3619.17	3619.10	3618.80	0.37	0.30
21	3769.75	3769.86	3769.35	0.40	0.51
<b>MAE:</b>	0.28	0.44			

Table S25: VPT2 anharmonic frequencies (in  $\text{cm}^{-1}$ ) of  $\text{CH}_3\text{CONH}_2$  calculated using PhysNet (NN1 and NN2) trained on MP2 data. They are compared to their reference *ab initio* values (MP2) as well as with experiment.<sup>8</sup> The MP2 frequencies are added as the VPT2 calculation is feasible in Gaussian. Only 20 modes are assigned. Note that four frequencies were obtained in argon matrix (269, 427, 1432, 1433).

Mode	NN1(MP2)	NN1(MP2)	MP2	Exp
1	-2337.85	-2548.69	-2425.72	–
2	-206.36	-204.12	-213.48	269.00
3	453.25	457.15	451.29	427.00
4	479.72	473.40	477.92	507.00
5	574.42	576.91	574.20	548.00
6	701.19	706.62	700.92	625.00
7	839.33	840.76	840.39	858.00
8	981.95	984.00	979.28	965.00
9	1037.24	1038.03	1033.17	1040.00
10	1056.99	1054.48	1054.59	1134.00
11	1342.26	1344.85	1340.62	1319.00
12	1370.49	1370.80	1371.24	1385.00
13	1444.48	1443.41	1443.50	1432.00
14	1464.30	1459.85	1463.58	1433.00
15	1556.28	1556.57	1552.95	1600.00
16	1718.97	1726.61	1725.92	1733.00
17	2996.35	2990.34	2994.98	2860.00
18	3005.78	2993.60	3008.41	2900.00
19	3068.72	3072.59	3070.81	2967.00
20	3496.12	3504.90	3501.75	3450.00
21	3646.50	3665.08	3657.46	3550.00
<b>MAE:</b>	47.23	48.40		

### 3 Transfer learning

#### 3.1 H<sub>2</sub>CO

**Table S26:** Normal mode frequencies of H<sub>2</sub>CO calculated from a TL model trained on CCSD(T)-F12 data and compared to their reference *ab initio* values. All frequencies are given in cm<sup>-1</sup>.

NN(TL)	CCSD(T)-F12	\Delta
1186.45	1186.53	0.08
1268.20	1268.08	0.12
1532.73	1532.67	0.06
1776.55	1776.53	0.02
2934.04	2933.75	0.29
3006.04	3005.75	0.29

**Table S27:** VPT2 anharmonic frequencies of H<sub>2</sub>CO calculated using a TL PhysNet model trained on CCSD(T)-F12 data. They are compared with experiment.<sup>1</sup> All frequencies are given in cm<sup>-1</sup>.

NN(TL)	Exp	\Delta
1167.39	1167.00	0.39
1244.93	1249.00	4.07
1497.82	1500.00	2.18
1745.22	1746.00	0.78
2770.34	2782.00	11.66
2820.39	2843.00	22.61

## 3.2 TL: Energy- and force-errors

Table S28: Out-of-sample errors of the TL models to CCSD(T) quality. The energy errors are given in kcal/mol and the force errors are given in kcal/mol/Å.

	NN(TL)			
	CH <sub>3</sub> CHO	CH <sub>3</sub> NO <sub>2</sub>	CH <sub>3</sub> COOH	CH <sub>3</sub> CONH <sub>2</sub>
EMAE:	0.0196	0.0228	0.0027	0.0097
ERMSE:	0.0197	0.023	0.0029	0.0099
FMAE:	0.0119	0.0183	0.0103	0.0161
FRMSE:	0.0307	0.0366	0.0188	0.0401



### 3.3 CH<sub>3</sub>CHO

Table S29: Normal mode frequencies (in cm<sup>-1</sup>) of CH<sub>3</sub>CHO calculated from a TL model trained on CCSD(T) data and compared to their reference *ab initio* values.

NN(TL)	CCSD(T)	\Delta
158.34	157.97	0.37
503.66	503.57	0.09
775.07	774.97	0.10
896.09	896.02	0.07
1130.36	1130.31	0.05
1136.02	1136.00	0.02
1388.27	1388.30	0.03
1420.92	1420.99	0.07
1474.26	1474.25	0.01
1484.77	1484.90	0.13
1777.53	1777.36	0.17
2919.35	2919.94	0.59
3030.98	3031.38	0.40
3098.85	3099.27	0.42
3150.54	3151.01	0.47

### 3.4 CH<sub>3</sub>NO<sub>2</sub>

Table S30: Normal mode frequencies (in cm<sup>-1</sup>) of CH<sub>3</sub>NO<sub>2</sub> calculated from a TL model trained on CCSD(T) data and compared to their reference *ab initio* values.

NN(TL)	CCSD(T)	\Delta
30.33	27.39	2.94
474.41	474.28	0.13
610.43	610.26	0.17
662.28	662.25	0.03
929.12	929.13	0.01
1114.68	1114.60	0.08
1144.23	1144.29	0.06
1410.41	1410.48	0.07
1425.35	1425.33	0.02
1477.67	1478.01	0.34
1490.72	1491.32	0.60
1613.79	1613.72	0.07
3082.80	3082.90	0.10
3179.75	3179.78	0.03
3207.18	3207.13	0.05

### 3.5 CH<sub>3</sub>COOH

Table S31: Normal mode frequencies (in cm<sup>-1</sup>) of CH<sub>3</sub>COOH calculated from a TL model trained on CCSD(T) data and compared to their reference *ab initio* values.

NN(TL)	CCSD(T)	\Delta
80.67	80.21	0.46
418.84	418.77	0.07
542.51	542.63	0.12
582.77	582.64	0.13
656.54	656.58	0.04
865.99	865.99	0.00
1006.75	1006.91	0.16
1073.32	1073.92	0.60
1216.03	1215.93	0.10
1347.96	1347.97	0.01
1421.21	1421.17	0.04
1484.75	1484.64	0.11
1491.69	1491.78	0.09
1816.71	1816.86	0.15
3059.07	3059.07	0.00
3131.34	3131.39	0.05
3175.04	3175.00	0.04
3756.19	3756.31	0.12

### 3.6 CH<sub>3</sub>CONH<sub>2</sub>

Table S32: Normal mode frequencies (in cm<sup>-1</sup>) of CH<sub>3</sub>CONH<sub>2</sub> calculated from a TL model trained on CCSD(T) data and compared to their reference *ab initio* values.

NN(TL)	CCSD(T)	\Delta
45.28	47.22	1.94
250.38	240.57	9.81
419.92	418.61	1.31
511.15	511.53	0.38
550.94	551.26	0.32
641.74	639.95	1.79
853.02	853.02	0.00
985.36	984.86	0.50
1058.77	1059.14	0.37
1128.27	1127.94	0.33
1345.44	1345.26	0.18
1411.63	1411.86	0.23
1484.27	1484.28	0.01
1500.92	1500.59	0.33
1630.04	1630.02	0.02
1768.18	1768.24	0.06
3046.36	3045.80	0.56
3119.82	3118.47	1.35
3156.39	3157.45	1.06
3594.26	3595.34	1.08
3730.94	3732.00	1.06

## 4 Scaled harmonic frequencies

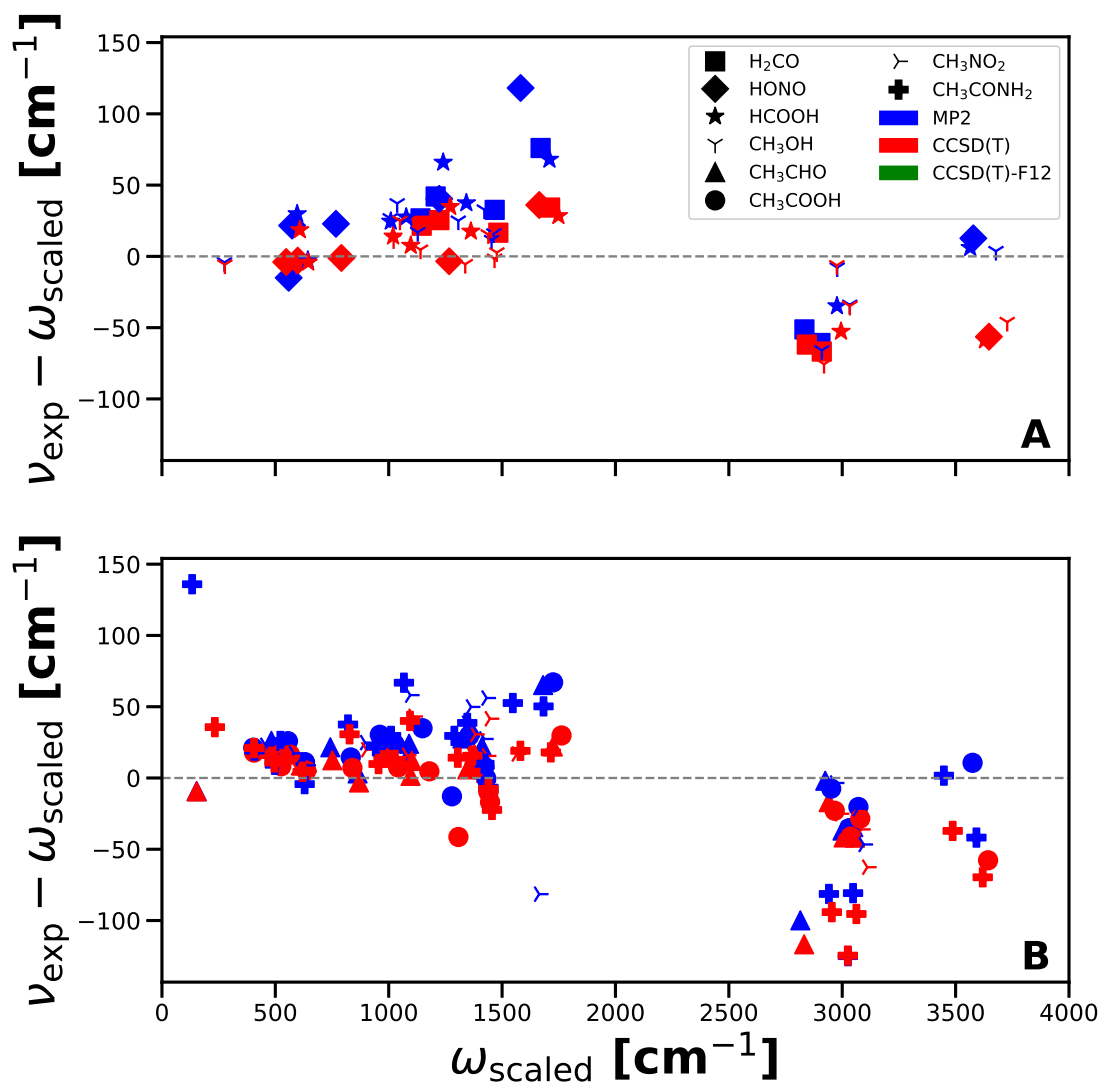


Figure S1: The accuracy of the scaled *ab initio* harmonic frequencies is shown with respect to the experimental values. The figure is divided into two windows for clarity.

## References

- (1) Herndon, S. C.; Nelson Jr, D. D.; Li, Y.; Zahniser, M. S. Determination of line strengths for selected transitions in the  $\nu_2$  band relative to the  $\nu_1$  and  $\nu_5$  bands of H<sub>2</sub>CO. *J. Quant. Spectrosc. Radiat. Transf.* **2005**, *90*, 207–216.
- (2) Guilmot, J.; Godefroid, M.; Herman, M. Rovibrational parameters for trans-nitrous acid. *J. Mol. Spectrosc.* **1993**, *160*, 387–400.
- (3) Tew, D. P.; Mizukami, W. Ab initio vibrational spectroscopy of cis- and trans-formic acid from a global potential energy surface. *J. Phys. Chem. A* **2016**, *120*, 9815–9828.
- (4) Serrallach, A.; Meyer, R.; Günthard, H. H. Methanol and deuterated species: infrared data, valence force field, rotamers, and conformation. *J. Mol. Spectrosc.* **1974**, *52*, 94–129.
- (5) Wiberg, K. B.; Thiel, Y.; Goodman, L.; Leszczynski, J. Acetaldehyde: Harmonic Frequencies, Force Field, and Infrared Intensities. *J. Phys. Chem.* **1995**, *99*, 13850–13864.
- (6) Goubet, M.; Soulard, P.; Pirali, O.; Asselin, P.; Réal, F.; Gruet, S.; Huet, T. R.; Roy, P.; Georges, R. Standard free energy of the equilibrium between the trans-monomer and the cyclic-dimer of acetic acid in the gas phase from infrared spectroscopy. *Phys. Chem. Chem. Phys.* **2015**, *17*, 7477–7488.
- (7) Wells, A.; Wilson Jr, E. B. Infra-Red and Raman Spectra of Polyatomic Molecules XIII. Nitromethane. *J. Chem. Phys.* **1941**, *9*, 314–318.
- (8) Ganeshsrinivas, E.; Sathyanarayana, D.; Machida, K.; Miwa, Y. Simulation of the infrared spectra of acetamide by an extended molecular mechanics method. *J. Mol. Struct.* **1996**, *361*, 217–227.